Title

Extended Phase I Study: Geophysical Investigation Survey Report - Las Animas Geophysical Study, Hollister to Gilroy 4 Lane, San Benito and Santa Clara Counties.

Authors

Hildebrand, John

Wiggins, Sean

Driver, Jeana

et al.

Publication Date

2003-06-01

Extended Phase I Study: **Geophysical Investigation Survey Report: Las Animas Geophysical Study, Hollister to Gilroy 4 Lane, San Benito and Santa Clara Counties**

District 5, Sbt-25 4 Lane Project
Contract 43A0088,
Task Order 1
EA 05-485400;
05-SBt-25 – KP 82.9/96.7 (PM 51.5/60.1)
04-SCl-25 – KP 0.0/4.1 (PM 0.0/2.5)
04-SCl-101- KP 1.0/8.2 (PM2.2/4.2)

Produced for: Dr. Mike McCoy, UCD
Dept. of Environmental Science and Policy
Under subcontract to CALTRANS, Tom Wheeler

John A. Hildebrand, Sean M. Wiggins
Jeana L. Driver and Allan W. Sauter
Scripps Institution of Oceanography
University of California, San Diego

Lawrence B. Conyers, Michael Grealy
and James Conyers
Geophysical Investigations Inc.
University of Denver
Denver, Colorado

USGS Chittenden Quadrangle map, 7.5 minute, 1955, photorevised 1980
(Tom: Township 11 S and Range 4 E.)
P-43-000315; CA-SCl-308/H; P-43-001077; CA-SCl-697/H)
Location key words: Gavilan Junior College, Gilroy
Resource key words: historic-period cemetery, Spanish/Mexican period rancho, adobe ranch house, geophysical testing, American-Period farm, Henry Miller

June 2003

Executive Summary

Caltrans, in cooperation with the Federal Highway Administration (FHWA), proposes to upgrade Highway 25, the Highway 25/101 interchange north of Hollister and south of Gilroy in San Benito and Santa Clara Counties and construct a Highway 25/156 interchange north of Hollister in San Benito County. Two related archaeological sites: the Miller Cemetery site (CA-SC1-308/H) and the Bloomfield Ranch site (CA-SCL-697H), are located in the southwest and southeast corners of the intersection of State Highways 25 and 101. Both sites contain historic and prehistoric components that may include human remains. The Las Animas geophysical study was carried out near the intersection of state Highways 25 and 101. This study was conducted to identify the locations for the Mariano Castro adobe foundations, the Henry Miller house foundations, and other historic and prehistoric features including human burials in compliance with 36 CFR Part 800.

This survey was designed to employ geophysical techniques that included three technical approaches: ground penetrating radar (GPR), total field magnetometry (MAG), and electromagnetic induction (EM). Only two of the geophysical tools were used, EM and GPR. Upon inspecting these locations, it was decided that MAG would not be effective because of the high metal content of the proposed survey area, and therefore it was not used.

Geophysical mapping in the Las Animas study area has located possible historic features buried by as much as a meter of sediment and soil. GPR reflection profiles and time-slice maps showed the location of four possible buried features in the 12 grids of data that were collected. The most promising of these features is located in GPR Grid 1-4 (EM B5, 6, and 7), at the Miller Cemetery site. The GPR feature is well correlated with an EM anomaly, which shows lower conductivity material to the south and east of the GPR feature. This material may be melted adobe from the Mariano Castro house structure or other early 19th century historic residence and is well correlated with appropriate time period pottery sherds found by Julia Costello and excavation results referred to in her report (Costello, 2002). Another possible buried building foundation was located in GPR Grid 1-6 at the Bloomfield Ranch site, just north of the "grassy knoll" near the Miller house. Two other, less well-defined and more problematic, features are located in the depression north of the Miller house and to the east in the agricultural field.

We suggest that subsurface testing is warranted at least for the Miller Cemetery Grid 1-4 anomaly and the Bloomfield Ranch Grid 1-6 anomaly to determine if they are associated with historic structures. Lower priority targets for testing are the Bloomfield Ranch Grid 1-5 and Grid 1-2. The overlay of modern objects and features at the Bloomfield Ranch house made a significant contribution to the geophysical anomalies at this site and may have obscured signatures from the older Mariano Castro adobe. On the other hand, the Miller Cemetery site is relatively less disturbed and yielded both geophysical anomalies and surface pottery that is consistent with a Spanish period occupation.

Geophysical Investigation Survey Report: Las Animas Geophysical Study, Hollister to Gilroy 4 Lane, San Benito and Santa Clara Counties

Produced for: Dr. Mike McCoy, UCD
Dept. of Environmental Science and Policy
Under subcontract to CALTRANS, Tom Wheeler

John A. Hildebrand, Sean M. Wiggins
Jeana L. Driver and Allan W. Sauter
Scripps Institution of Oceanography
University of California, San Diego

Lawrence B. Conyers, Michael Greely
and James Conyers
Geophysical Investigations Inc.
University of Denver
Denver, Colorado

Introduction

Caltrans, in cooperation with the Federal Highway Administration (FHWA), proposes to upgrade Highway 25, the Highway 25/101 interchange north of Hollister and south of Gilroy in San Benito and Santa Clara Counties and construct a Highway 25/156 interchange north of Hollister in San Benito County. Two related archaeological sites: the Miller Cemetery site (CA-SC1-308/H) and the Bloomfield Ranch site (CA-SCL-697H), are located in the southwest and southeast corners of the intersection of State Highways 25 and 101. Both sites contain historic and prehistoric components that may include human remains. The Bloomfield Ranch was originally a part of the Rancho Las Animas, a land grant confirmed to Mariano Castro between 1808 and 1810. Castro constructed an adobe house on the property in the early 1800s. The Rancho Las Animas was purchased in 1859 by Henry Miller. Miller constructed a large house on this site in the early 1870s which subsequently burned down in 1923. The Bloomfield Ranch is one of two suggested locations for the site of the Mariano Castro adobe. The other is the Miller Cemetery site where remnants of the Miller family cemetery are located, including a stone and metal fence but lacking inhumations which are reported to have been relocated.

The Las Animas geophysical study was carried out near the intersection of state Highways 25 and 101. This study was conducted to identify the locations for the Mariano Castro adobe foundations, the Henry Miller house foundations, and other historic and prehistoric features including human burials in compliance with 36 CFR Part 800.

The area in and around the Bloomfield Ranch site is located in the Carnadero River valley bottom. The area was identified during archival research of historic documents, including land grants and subsequent deeds that indicate this was the original location of the adobe complex (Wee, 2002). The Bloomfield Ranch site is presently occupied by several modern houses, garages, storage sheds and other cultural features. In geophysical terms the site is "noisy" because there are an abundance of buried pipes, overhead power and other utility lines, and the ground has seen a great deal of compaction and disturbance from trucks and agricultural plowing.

The second area of interest is the Miller Cemetery site, located on a bluff northwest of the Bloomfield Ranch site. This cemetery is walled with stone, capped by an iron fence and is now used as an enclosure for cattle. Other areas surrounding the cemetery wall have been fenced with barbed wire. Reconnaissance surveys by Julia Costello discovered pottery sherds at this site dating from the time of the postulated Mariano Castro adobe structure, brought up in rodent burrows just south of the cemetery. The potential for an historic structure based on these findings

as well as test excavations in 1993 (Costello, 2002) made this site a target for geophysical mapping.

Geophysical Techniques

This survey was designed to employ geophysical techniques that included three technical approaches: ground penetrating radar (GPR), total field magnetometry (MAG), and electromagnetic induction (EM). Only two of the geophysical tools were used, EM and GPR. It was decided that MAG would not be effective because of the high metal content of the proposed survey areas, and therefore was it not used.

GPR mapping can produce images of changes in soil and sediment stratigraphy and these images are generally not influenced by most types of buried metal. GPR, however, is slower to collect and therefore less ground can be surveyed per day than can be accomplished with EM. EM is a useful tool for mapping soil changes, including adobe content which potentially could be used to identify the location of the Mariano Castro adobe. This device is influenced by metal and its data can produce maps of buried metal pipes and other objects.

GPR and EM grids were laid out using the baselines established in July 2002 (Costello, 2002), as anchor points. Grids were designed to cover as much of the area around the baselines as possible while taking into account site characteristics. A total area of 14,000 m^2 was surveyed with GPR during five days of field work and 16,000 m^2 with EM, collected over 7 days of field work.

GPR Mapping

Ground-penetrating radar data are gathered by transmitting pulses of radar energy into the ground from a surface antenna, reflecting the energy off buried objects, features, or bedding contacts and then detecting the reflected waves back at the ground surface with a receiving antenna. When collecting radar reflection data, antennas are moved along the ground surface in line transects within a grid. As radar waves penetrate the ground, they move through various materials, and the velocity of the waves may change depending on the physical and chemical properties of the materials through which they are traveling (Conyers and Goodman 1997: 31-40). The greater the contrast in electromagnetic properties between two materials at an interface, the stronger the reflected signal, and therefore the greater the amplitude of reflected waves received at the surface (Conyers and Goodman 1997: 33-34). When travel times of reflected energy pulses are measured, and their velocity through the ground is known, distance (or depth in the ground) can be accurately measured (Conyers and Lucius 1996). Each time a radar pulse traverses a material with a different composition or water saturation, the velocity will change and a portion of the radar energy will reflect back to the surface and be recorded. The remaining energy will continue to pass into the ground to be further reflected, until it finally dissipates with depth.

The ability of GPR to image objects and structures is dependent on soil and sediment mineralogy, clay content, ground moisture, depth of burial and surface topography and vegetation. Electrically conductive or highly magnetic materials will quickly dissipate radar energy and prevent its transmission to depth. The best conditions for energy propagation are dry sediments and soil, especially those without an abundance of clay. Soil types in the Gilroy area are a mixture of sand and sandy-silty loam. Radar energy was easily transmitted through the sand, even when moist, and produced distinct reflections at buried interfaces. Quality of the radar reflections was somewhat influenced by the ground surface, with recently plowed areas producing the poorest quality data and compacted areas the best.

The depth to which radar energy can penetrate and the expected subsurface resolution are partially controlled by the frequency (and wavelength) of the radar energy transmitted (Conyers and Goodman 1997: 40-52). Standard GPR antennas propagate radar energy that varies in frequency from about 10 megahertz (MHz) to 1000 MHz. Low frequency antennas (10-120 MHz) generate long wavelength radar energy that can penetrate up to 50 m in certain conditions, but are capable of resolving only large buried features. In contrast, the maximum depth of penetration of a 900 MHz antenna is about one meter or less in typical soils, but can resolve reflected features on the scale of a few centimeters. A trade-off therefore exists between depth of penetration and subsurface resolution. In the Las Animas surveys the 400 MHz and 900 MHz antennas were used, which resolved features as small as about 0.10 m in diameter at depths up to about 1.5 m with the 900 MHz antenna.

EM Induction Mapping:

Electromagnetic (EM) fields are composed of both an electrical and a magnetic wave that propagate 90 degrees out of phase. When that field encounters buried materials that are either electrically conductive or magnetically susceptible a secondary field is generated (Reynolds 1997). This secondary field is then detected and measured by a receiving coil, located at the surface a fixed distance from the source coil. As the EM coils are moved along the ground surface in transects, changes in the secondary field can be measured. These electromagnetic induction measurements detect changes in the physical and chemical properties of underlying sediments and soils.

Two properties are measured, the electrical conductivity and the magnetic susceptibility (Reynolds 1997), obtained respectively from the out-of-phase and in-phase response to the transmitted energy. A lateral change in soil properties from dry sand, which is not very electrically conductive, to moist clay that is conductive, will change the electrical (out-of-phase) component of the EM field, while the distribution of buried metals, which have high magnetic susceptibility, will influence the magnetic (in-phase) portion of the EM field. These changes will be recorded by the surface instrument, and if many measurements are taken within a grid, the discontinuity between two buried materials can be mapped. Due to the high concentration of modern metal in the survey areas, the magnetic susceptibility (in-phase signal) was not used. We recorded the electrical (out-of-phase) component of the field and mapped these data along a series of transect lines to reveal changes in subsurface electrical conductivity.

Most soil and sediments are poor electrical conductors, and therefore higher readings are primarily a function of changes in water saturation, the porosity of the materials, concentration of dissolved electrolytes, the temperature and chemical state of the pore water and the amount and types of clays that are present. If the water in the pore spaces contains dissolved electrolytes, then the changes in the porosity or permeability will be reflected in electrical conductivity measurements. Electricity will pass through wet clay units easier than wet sands, and this higher electrical conductivity will be measured at the surface. Different types of clay also have different conductivities, depending on their mineralogy, that can affect the readings. While clay is generally expected to have a high conductivity, it has been our experience that adobe produces low conductivity readings relative to surrounding soils. This could be due to a difference in electrolyte content caused by firing or other changes to the clay composition produced during the adobe making process.

Buried metal objects as well as pipes, metal fences and other recent cultural materials affected the data quality in most of the grids. The EM data showed changes in soil characters in each of the grids, possibly denoting areas of varying clay and sand content from sandier areas. This kind of information is important when attempting to delineate areas of old adobe architecture, where the adobe has melted and become incorporated into the soils. The abundance of metal features in some of the grids at the Bloomfield Ranch site partially obscured more subtle changes in soil properties.

Methods

Two data collection trips were conducted for the Las Animas project: (a) July 10-13, 2002, and (b) October 18-19, 2002. During both trips GPR and EM data were collected (Tables 1 and 2).

GPR Data Collection and Processing

The GPR system used for the project was a Geophysical Survey Systems Inc. (GSSI) Subsurface Interface Radar (SIR) 2000 model. The GPR antennas used for the testing were dual 400 and 900 MHz frequency antennas that produce a radar pulse of about 35 and 15 cm in wavelength respectively.

Two types of images can be produced from GPR data: time-slice maps and vertical profiles. Time-slice maps image the amplitudes of reflections that arrive at a specified time within a grid. These can later be interpreted as horizontal maps of features at a given depth. Vertical profiles are images of all the reflections received along a single transect. These can be interpreted as a two-dimensional cross-section along the antenna track. Time-slice map views are often able to produce images of architectural features that do not show up well in vertical profile, while sometimes the inverse is true.

The time window during which the system recorded reflections ranged from 20 to 40 nanoseconds, depending on the targets to be imaged and the ground conditions in each grid. The greater the time window, the deeper the system can potentially record reflections, however, radar energy dissipation limits the realized depth of recorded reflections. Calculations were made in advance to determine the "footprint" of the GPR energy at the depth necessary to image the features of interest (Conyers and Goodman 1997: 36). Using both the 400 and 900 MHz antennas, and with velocities calculated in the field, a 0.5 m line spacing produced complete coverage of the subsurface. Data were collected in the October 2002 trip using a survey wheel, which normalized the distance between reflection traces. One reflection trace was collected every 4 cm along each transect, producing a dense series of data in the profiling direction. The lengths of the lines were altered throughout the grids in order to cover as much area as possible and grids were not always rectangular. Reflection data in the grids collected in July, 2002, were gathered using a manual survey marker, which allowed line lengths to be altered during collection to avoid surface obstacles.

Descriptions of GPR grids are shown in Table 1. Outlines of the GPR grids, overlain on aerial photos are shown in Figure 1 for the Bloomfield Ranch site and Figure 2 for the Miller Cemetery site. A red circle marks the origin of each grid while an arrow indicates the direction of the first profile. The initial profile direction for grid 1-5 is indicated by a yellow arrow. All GPR reflection data were collected as 16 bit data, with 512 samples defining each trace. Grids 1-6 and 1-7 were collected with the 900 MHz antenna. All other grids were collected with the

400 MHz. The data were frequency filtered to remove extraneous noise from the reflection traces. Range gains were applied in the field to enhance deeper reflections. Range gains were modified for each surface material and for the ground conditions encountered at the time of collection. The parameters are stored in the header of each raw data file.

Table 1: GPR grid data description

GPR Grid	Data name	Location	Date collected	Lines	Maximum size	Origin
1-1	07_10_02	North, west and south of Miller house	7/10/02	76	75x60 m	NW
1-2	07_10_02.001	East of Miller house in the lettuce field	7/10/02	19	40x18 m	SW
1-3	07_11_02	Outside of cemetery fence	7/11/02	51	45x50 m	SW
1-4	07_11_02.001	Inside cemetery fence	7/11/02	37	40x37 m	SW
1-5	07_12_02	Depression N of Miller House	7/12/02	30	27x29 m	SW
1-6	07_12_02.001	North of Miller house (900 MHz)	7/12/02	81	20x29 m	NE
1-7	07_13_02	Depression N. of Miller house (900 MHz)	7/13/02	108	28x30 m	SW
2-1	10_18_02	South of S. garage Miller house	10/18/02	34	16x55 m	NW
2-2	10_18_02.001	East of Grid 1: Miller house	10/18/02	26	13x55 m	NW
2-3	10_19_02	East of S. Garage: Miller house	10/19/02	21	10x28 m	SW
2-4	10_19_02.001	North of Grid 3: Miller house	10/19/02	21	10x32 m	SW
2-5	10_19_02.002	North end of Grid 3: Miller house	10/19/02	26	12.5x30 m	NW
2-6	10_19_02.003	North end of Grid 4: Miller house	10/19/02	21	10x30 m	NW

All GPR reflection data were first analyzed as vertical profiles in two-dimensions to determine the nature of subsurface reflections: their wavelength, depth of penetration, amount and nature of background interference, and the velocity of radar energy in the ground (see Appendix 1 for selected GPR vertical profiles at 2m line spacing). The data from all surveys, except the newly plowed lettuce field (Figure 1: Grid 1-2), the "grassy knoll" area (Figure 1: 1-6) and the depression north of Miller house (Figure 1: 1-7) were of exceptionally high quality due to the lack of conductive materials and the abundance of sand in the soil.

To determine the depth of penetration and energy attenuation, velocity studies were conducted on radar profiles from each grid. This is done using a computer program called *Fieldview*, which can quickly calculate the geometry of hyperbolic radar reflections in the ground. Hyperbolic reflections are produced from buried "point sources" such as rocks, pipes, walls or other discrete features. The velocity of the surrounding material will affect the geometry of the hyperbola, and when a model curve is "fit" to the hyperbola in the ground, velocity can be calculated. This was done for point sources in each of the three study areas and velocity was calculated at a number of different depths. All velocities were surprisingly consistent. The relative dielectric permittivity (RDP) ranged from 7 to 8 which indicates that each 2 nanoseconds of two-way GPR travel is equal to about 0.10 m in the ground.

EM Data Collection and Processing

The instrument used for all EM surveys was the Geonics EM-38. The peak detection depth is determined by the separation between the transmitting and receiving coils. In the case of the EM-38 this depth is at 0.4m. EM data were collected at 0.5 m line spacing with measurements taken automatically every 0.4 seconds while traveling at walking speed. Fiducial marks in the data were placed manually every 5 m.

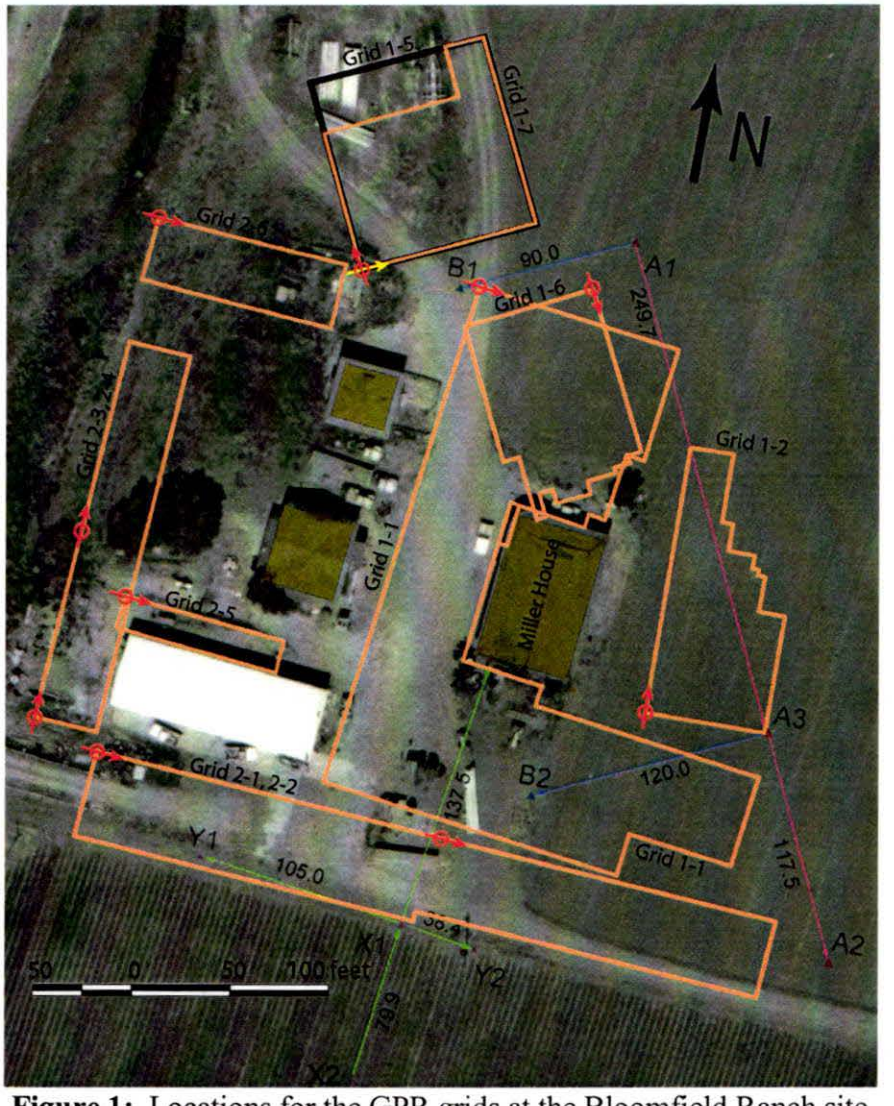

Figure 1: Locations for the GPR grids at the Bloomfield Ranch site.

The electrical conductivity data collected along each transect for each grid were first normalized in distance to provide equally spaced measurements between fiducial marks because walking rates vary. This was done by "rubber sheeting" each of the profiles between fiducial marks, sometimes stretching, and sometimes compacting the intervals between points. This provides an equal distribution of points for each grid. Data were then exported to an image production program (*Surfer*, v. 7, 1999) to produce maps of electrical conductivity for the grids.

Descriptions for each EM grid are shown in Table 2. The grids, overlain on aerial photos, are shown in Figures 3 and 4 for the Bloomfield Ranch and Miller Cemetery sites.

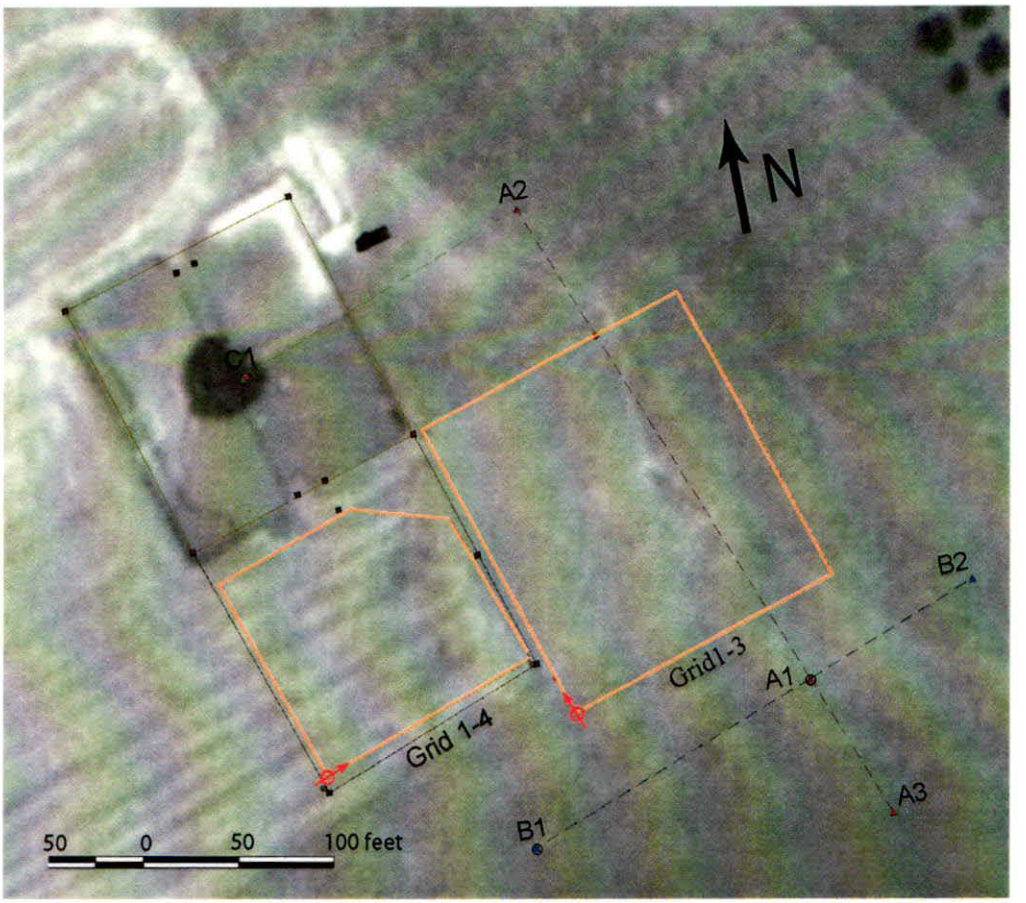

Figure 2: GPR grids superimposed on the aerial photo of the Miller Cemetery site. Grid 1-3 is outside the barbed wire fence and Grid 1-4 is within.

Table 2: EM grid data description

EM Grid	Data name	Location	Date collected	Maximum size
EM-A1	2101-2103.1	West of Miller house	7/11/02	14x57 m
EM-A2	2201-2205	South of Miller house	7/11/02	17x45 m
EM-A3	2301-2303	East of Miller house	7/11/02	7x35 m
EM-A4	2701-2706	North of Miller house	7/12/02	20x25 m
EM-A5	2601-2605	Depression North of Miller house	7/12/02	27x29 m
EM-A6	6001-6007	South of S. Garage: Miller house	10/18/02	30x55 m
EM-A7	5002-5008	East of EM-A6: Miller house	10/18/02	30x55 m
EM-A8	7001-7003	East of S. Garage: Miller house	10/19/02	10x28 m
EM-A9	8001-8005	North of EM-A8: Miller house	10/19/02	32x10 m
EM-A10	9001-9004	North end of EM-A8: Miller house	10/19/02	18.5x30 m
EM-A11	1101-1103	North end of EM-A9: Miller house	10/19/02	10x30 m
EM-B1	1101-1106	East of cemetery	7/8/02	25x40 m
EM-B2	12001-12010	South-east of cemetery	7/8/02	45x45.5 m
EM-B3	1301-1307	South of EM-B2	7/9/02	30x45 m
EM-B4	1401-1407	West of EM-B3	7/9/02	30x55 m
EM-B5	1501-1506	South of Cemetery	7/10/02	24.5x35.5 m
EM-B6	1601-1604	East of EM-B5, East of EM-B2	7/10/02	11.5x23 m
EM-B7	1701-1702	North of EM-B6	7/10/02	8.5x27 m
EM-B8	1801-1806	East of EM-B1	7/10/02	20x21 m
EM-B9	10901-10905	North of EM-B7, West of EM-B1	7/13/02	17x19 m

Production of Image Maps

Data from both the EM maps and GPR time slices were imported to *Surfer* to produce gridded maps and final images. Data points were interpolated between transect lines. The final images have colors assigned to denote high and low data values. For both GPR reflection amplitudes and EM electrical conductivity, blue and green colors were assigned to low values. The "hotter" colors such as red and yellow indicate higher data values.

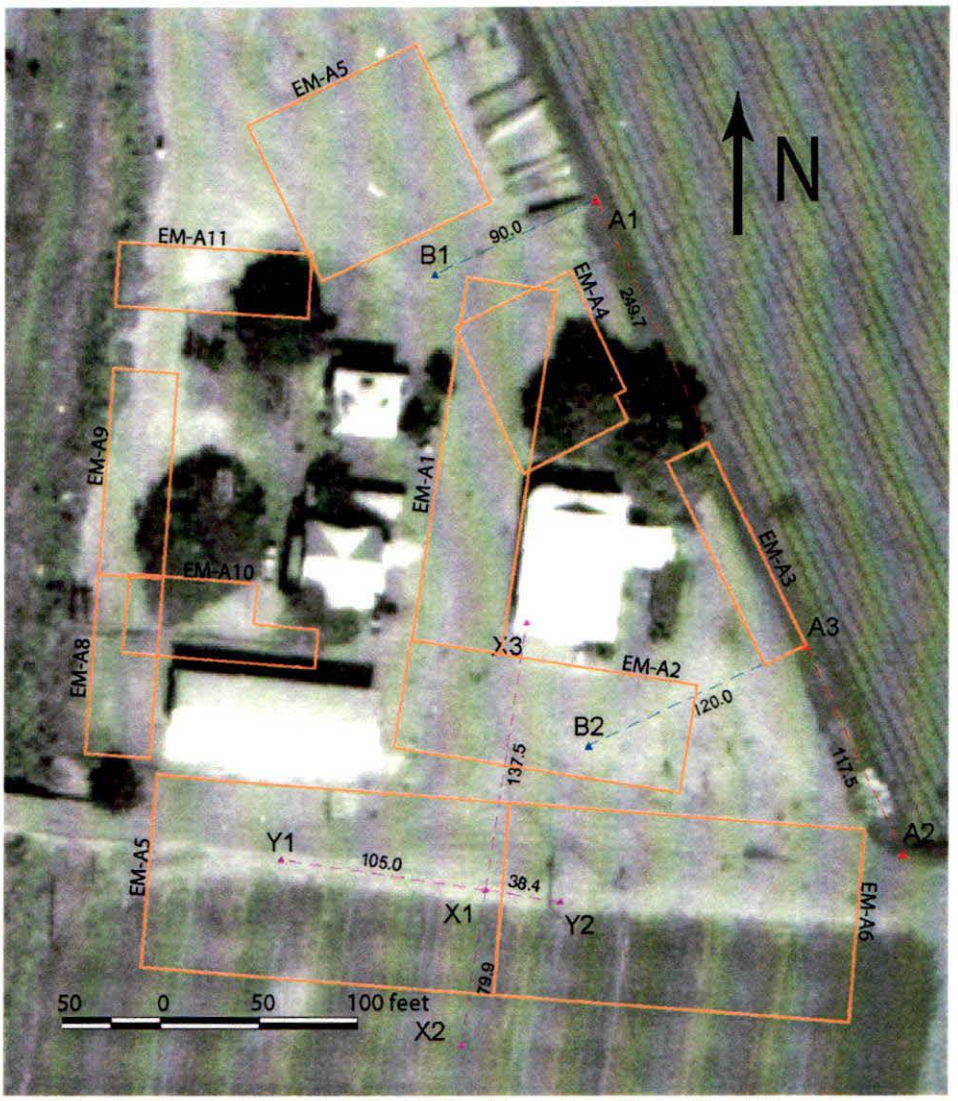

Figure 3: Locations for the EM grids at the Bloomfield Ranch site.

When the EM system crossed over shallow buried metal, the receiver coil was often saturated and produced very high and low readings. For example, a high-to-low-to-high "M" shape is observed when the EM38 crosses perpendicular to a metal buried pipe with the buried pipe located at the middle of the anomaly. On the EM maps, these readings often show up as white features or white with black at the center. In all cases the distribution and range of values for each of the colors were modified for each map to highlight features of interest. This provides a relative amplitude map to show relative differences but should not be interpreted as absolute values. GPR and EM maps of interest were overlain on aerial photos for each location.

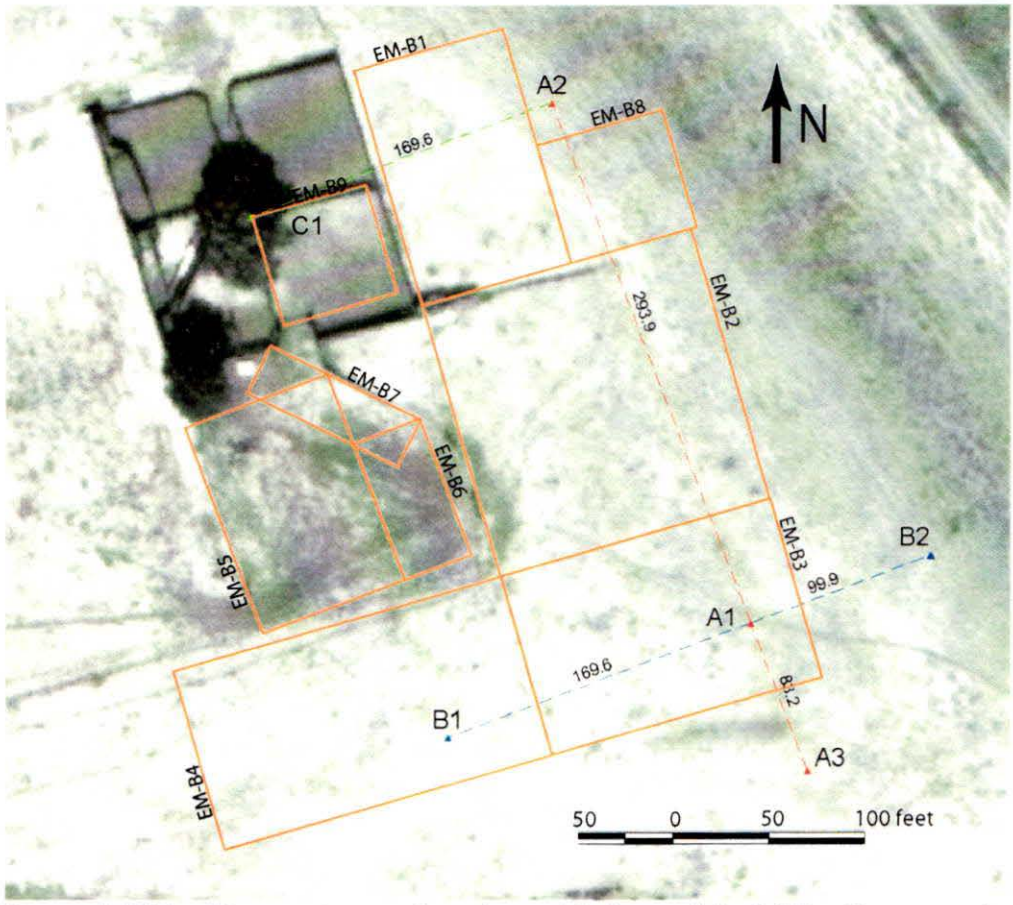

Figure 4: EM grids superimposed on the aerial photo of the Miller Cemetery site.

Results

Bloomfield Ranch Location

GPR 1-1 and EM-A1, A2, A4: These grids were collected primarily within the compacted dirt driveway between the two rows of houses at the Bloomfield Ranch location (Figures 1 and 3). A number of linear features are seen in the GPR images that denote the location of buried water or sewer pipes (Figure 5). They are visible trending parallel to the long axis of the grid. The EM maps (Figure 6) show at least 2 pipes, but in different locations than those seen in the GPR grids. It appears that the GPR and EM are producing images of different types of buried pipes. The GPR is probably mapping the larger non-metallic pipes such as ceramic or PVC sewer pipes while the EM is delineating the metal pipes. During data collection it was noticed that the EM signal was saturated throughout much of the grid by the buried metal in this area. This is visible in the EM maps, as much of the grid is colored white, indicative of saturated signals (Figure 6).

One buried feature was found in the grid, just north of the "grassy knoll" next to the propane tank. This area was re-surveyed in Grid 1-6 and will be discussed further below. No other buried archaeological or historical features were found in this grid, either in the GPR or EM data.

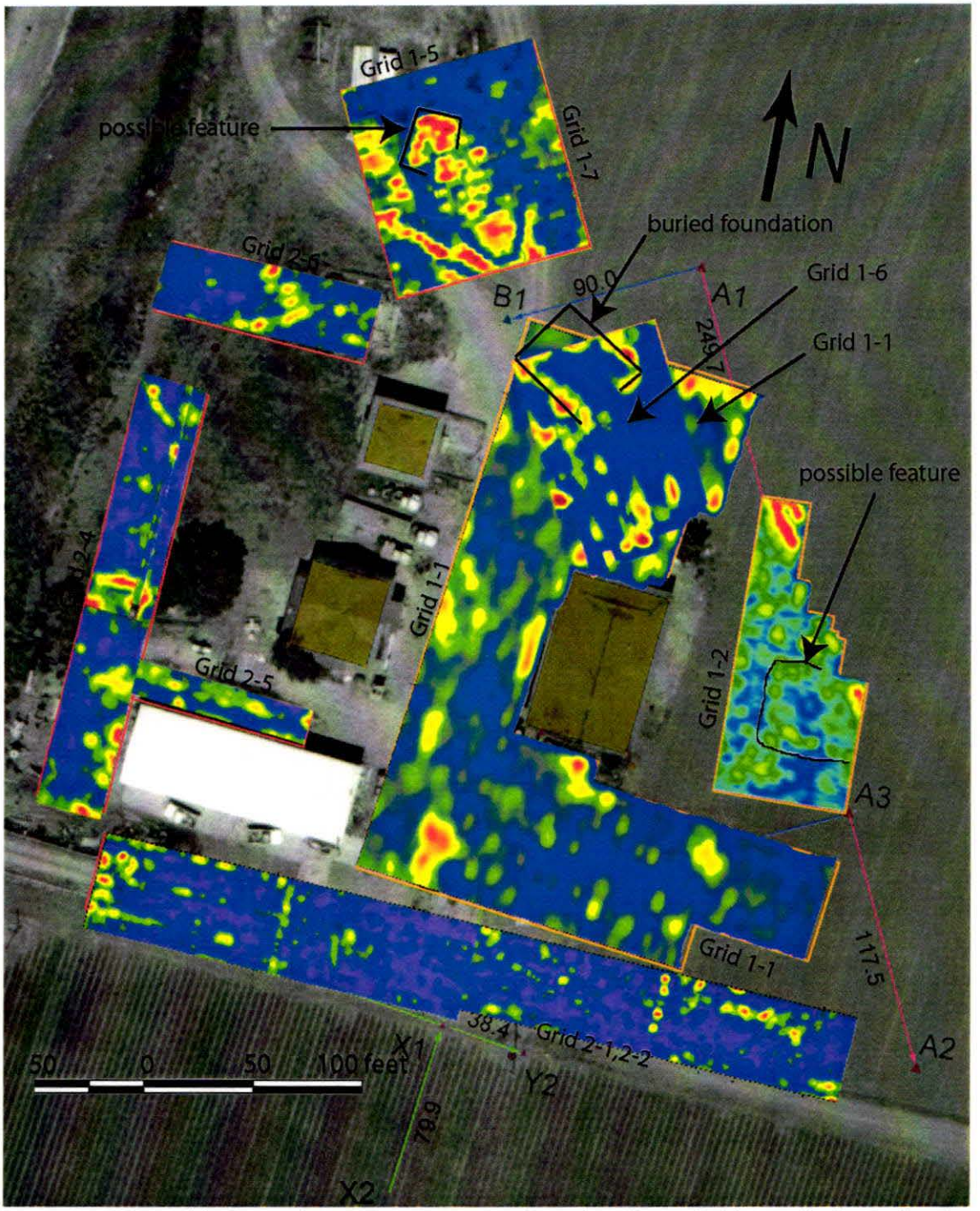

Figure 5: GPR grids from about 50-100 cm depth at the Bloomfield Ranch site indicating locations of possible buried structures and features.

GPR 1-2 and EM-A3: This grid, located to the east of the Miller house in a lettuce field (Figures 1 and 3), yielded poor quality data, probably because the field had been just harvested and then plowed, leaving ridges of un-compacted soil and deep furrows. There was poor coupling of the transmitted radar energy with the ground, producing "streaking" in the data. These streaks were partially filtered out of the profiles to produce the maps. There was

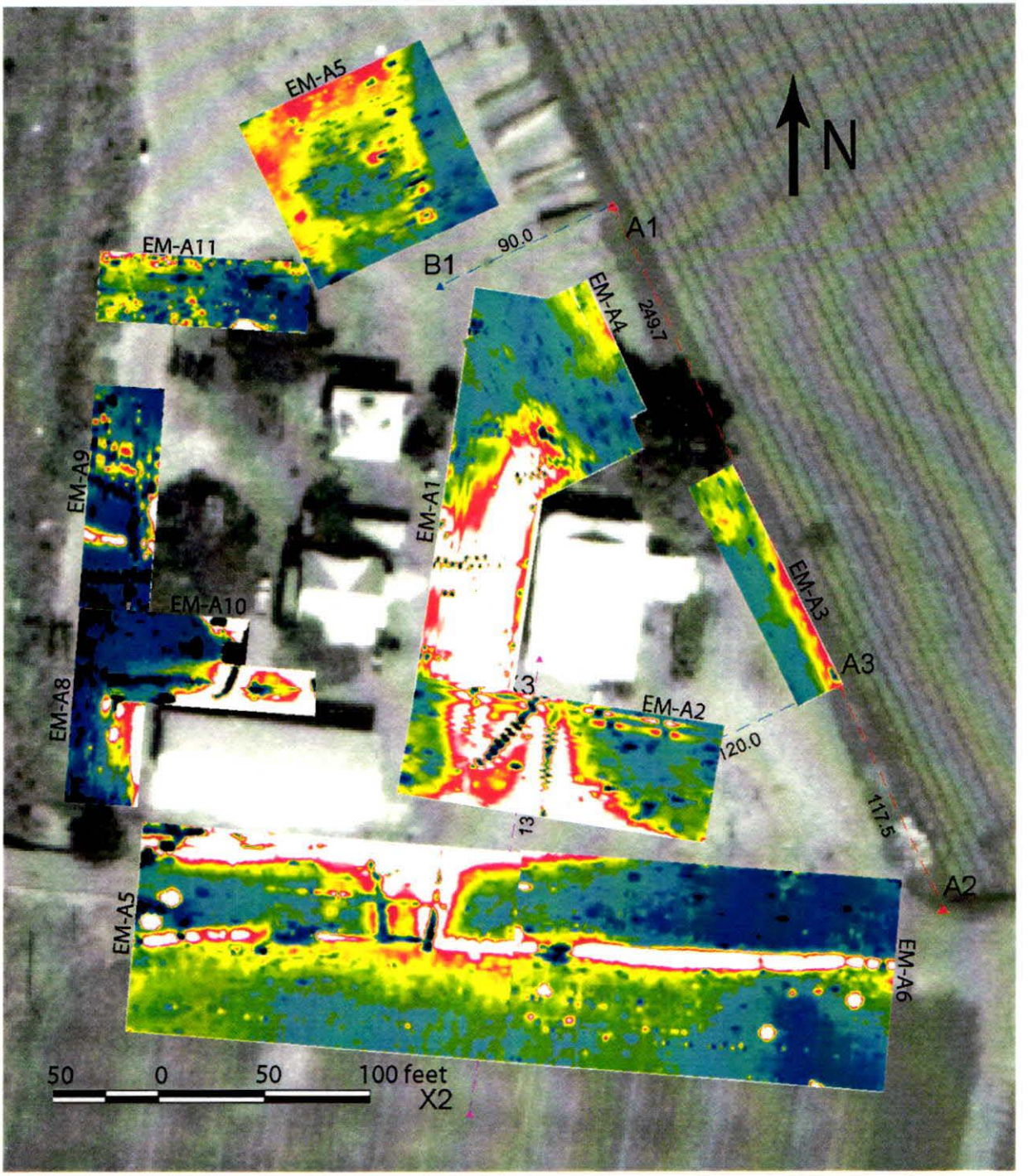

Figure 6: EM grids at the Bloomfield Ranch site.

one faint feature in the middle of the grid, defined by weak reflections that appeared rectangular when mapped (Figure 5). The two-dimensional profiles did not confirm the presence of this possible feature, and it is considered questionable at this time. The EM data did not delineate any features in this area (Figure 6).

GPR 1-5 and EM-A5: These grids of data were collected in a shallow depression north of the Miller house site, around which trucks are currently driven (Figures 1 and 3). The trucks had compacted the areas surrounding the depression and residual moisture had accumulated in the middle where the trucks do not drive. It was hypothesized that a depression

of this sort might be the surface expression of something lying underneath (perhaps a buried foundation or cellar), and therefore worthy of geophysical testing. The EM maps (Figure 6) showed some variations in electrical conductivity in this grid. A zone of low conductivity was seen as a patch in the middle and northern edge of the grid.

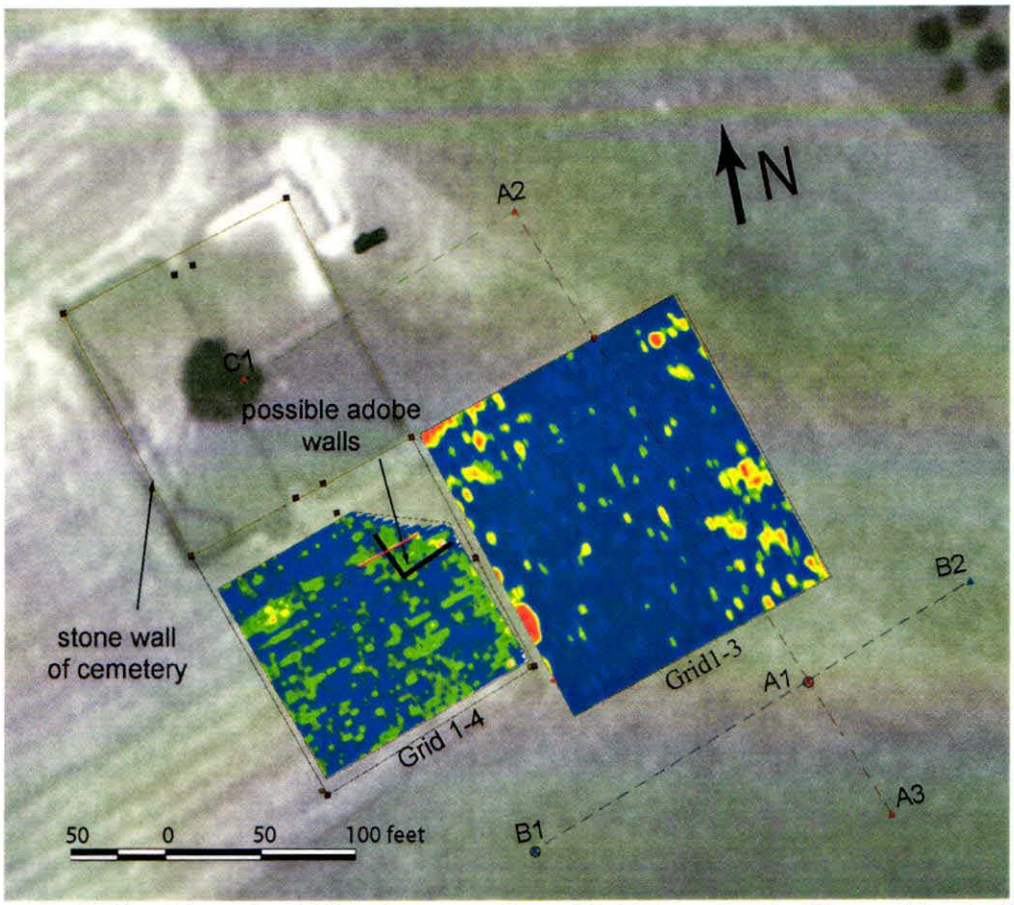

Figure 7: GPR grids at the Miller Cemetery from 50-100 cm depth. The red line indicates transect line #14 as shown in Figure 9.

The GPR maps show a square or rectangular feature within the middle of the depression, which might be a house foundation or collapsed basement (Figure 5). This feature occurs at about 80 cm to 1 m depth. The data in this grid suggest higher radar attenuation, probably because of the higher moisture content in the depression. A visual analysis of the two-dimensional profiles across this feature showed no walls or foundations. Time-slice map views are able to produce images of architectural features that do not show up well in vertical profile, although sometimes the inverse is true. In this case, there may be a structure in the time-slice maps that cannot be confirmed in the two-dimensional profiles.

GPR 1-7: This grid was collected in the same general location as grid 1-5, except the 900 MHz GPR antenna was used instead of the 400 MHz. It was hoped that the higher frequency energy from this antenna would better define the buried structure seen using the 400 MHz antenna. Unfortunately, 900 MHz energy was attenuated at a very shallow depth at this location, and no usable data were collected from the depth of the possible feature.

GPR 1-6 and EM-A4: A small grid of 900 MHz GPR data was collected on the "grassy knoll", an area just north of the Miller house near the propane tank (Figure 1). It was hypothesized that this small mound might be the remains of a structure. Some indications of a buried feature were seen in the 400 MHz data collected in Grid 1-1 in this area, and it was decided to re-collect the grid with the higher frequency 900 MHz antenna for better resolution. The GPR maps were able to delineate the foundation of a buried building, but surprisingly it was not under the knoll, but to the north on the margin of the parking lot (Figure 5). This buried feature appears to be a concrete or compacted dirt foundation to a building, located about 1 m below the ground surface. The EM signal is uniform across this region and does not suggest a buried feature (Figure 6).

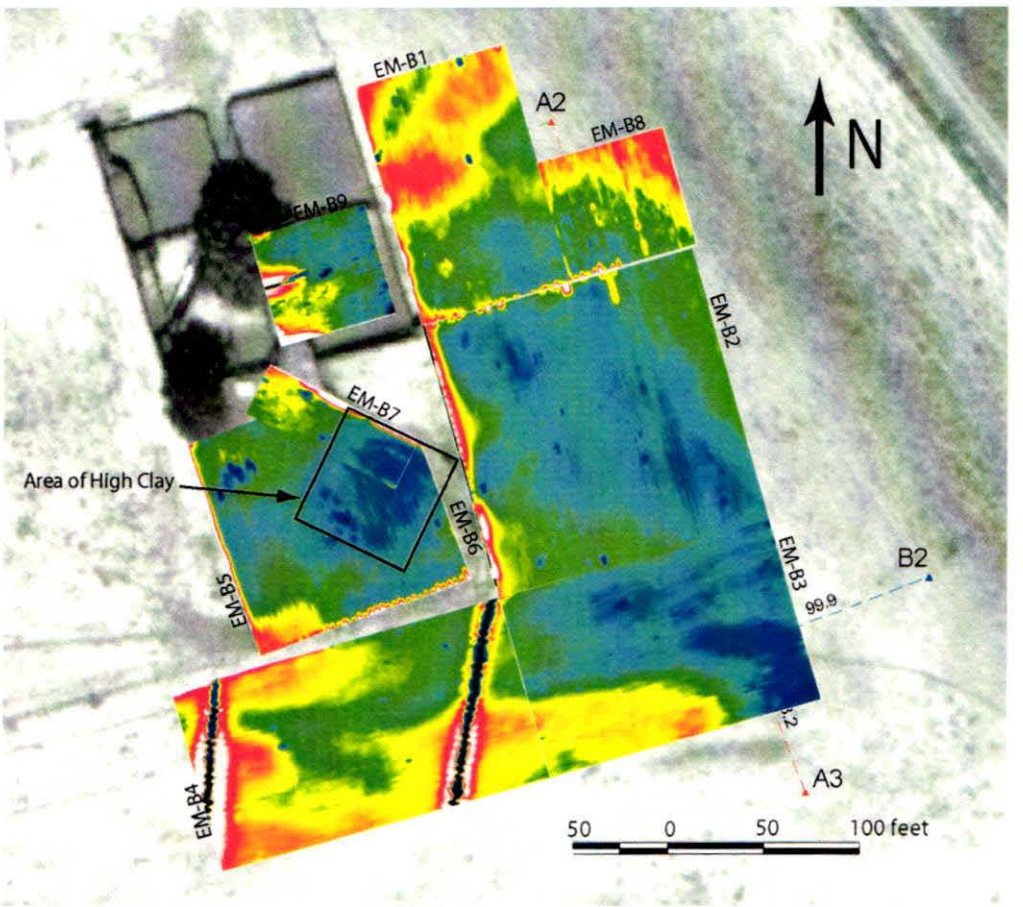

Figure 8: EM grids at the Miller Cemetery site.

GPR 2-1 through 2-6 and EM-A6 through EM-A11: These grids were located in all the open areas to the west, north and south of the Miller House and the other modern structures at the Bloomfield Ranch site (Figure 1 and Figure 3). Several linear features were discovered in these grids with both EM and GPR mapping (Figures 5 and 6), but all appear to be buried pipes. This area had an abundance of metal debris from agricultural machinery that affected the readings of both the EM and GPR systems. No apparent historical or archaeological features were identified in these areas.

Miller Cemetery Location

GPR 1-3 and EM-B2, B3, and B4: This grid is located southeast of the Miller Cemetery wall (Figures 2 and 4). Most of the GPR reflections that were found in this grid were probably produced from burrows or other soil disturbances, as none were correlative from profile to profile. This can be seen in the GPR maps from 50-100 cm depth (Figure 7), which shows some "point" reflections, but nothing that is spatially extensive. The EM data in grids B2, B3 and B4 easily mapped the buried metal water pipes that lead to the watering troughs (Figure 8). Broad regions of soil moisture variations may be revealed, especially in the southern portions of grids B3 and B4. There were no features visible in either the GPR or the EM maps in this grid that are suggestive of historical or archaeological features.

GPR 1-4 and EM-B5, B6, B7: This grid of data is located inside the barbed wire stock fence south of the cemetery (Figures 2 and 4). This is an area where Julia Costello reported historic pottery sherds in animal burrows, which date to about the time of the Mariano Castro adobe (Costello, 2002).

The GPR data in this grid show several reflections in the two-dimensional profiles that appear to be buried walls and floors (Figure 9). The location of the transect line #14 of Figure 9 is indicated with a red line in Grid 1-4 of Figure 7. Maps of the GPR data from depth where the wall reflections were visible (approximately 50 cm) showed possible wall foundations in the northeast corner of the grid (Figure 7). In approximately the same location, there is an area of low conductivity visible on the EM maps (Figure 8). This area is broader in extent than the possible wall features shown in the GPR data and may denote the location of melted adobe. It has been our experience that adobe and its melt produce low conductivity signatures, possibly due to changes that are produced in the clay during adobe construction. Both the EM and GPR maps suggest a buried feature in this grid, perhaps the historic Mariano Castro adobe. This area warrants further investigation by subsurface testing.

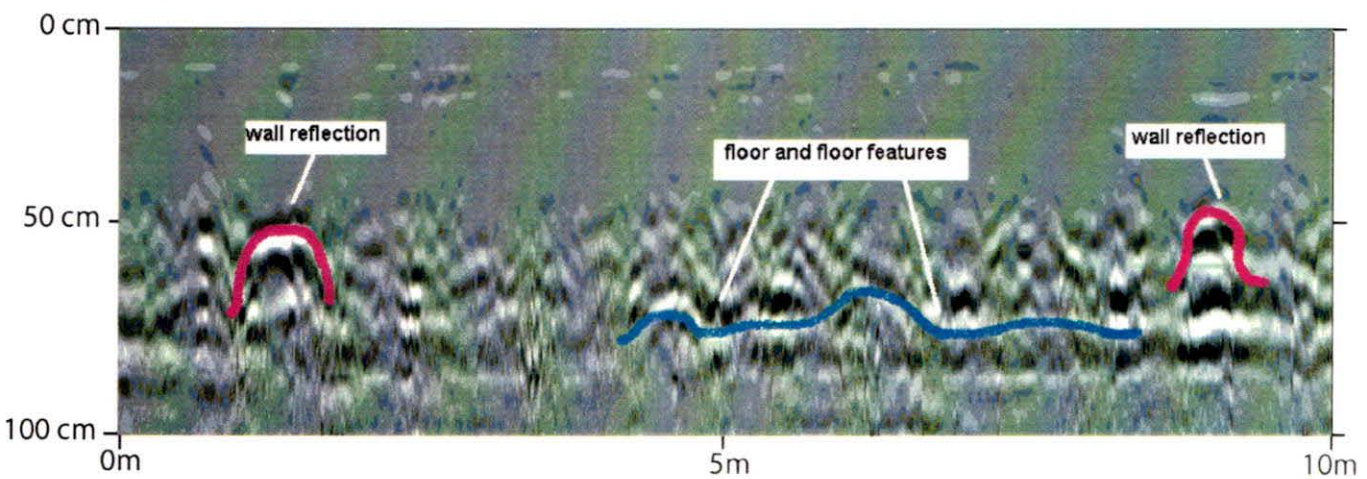

Figure 9: A GPR profile from the Miller Cemetery site, File 14 in Grid 1-4 located 7 m from the north edge of the grid, with a length of 10 m (see red line in Figure 7). Two significant wall reflections were discovered with a floor and possibly floor features between the walls.

Conclusion

Geophysical mapping in the Las Animas study area has located possible historic features buried by as much as a meter of sediment and soil. GPR reflection profiles and time-slice maps showed the location of four possible buried features in the 12 grids of data that were collected. The most promising of these features is located in GPR Grid 1-4 (EM B5, 6, and 7), at the Miller Cemetery site. The GPR feature is well correlated with an EM anomaly, which shows low conductivity material to the south and east of the GPR feature. This material may be melted adobe from the Mariano Castro house structure or other early 19th century historic residence and is well correlated with appropriate time period pottery sherds found by Julia Costello and excavation results referred to in Costello (2002). Another possible buried building foundation was located in GPR Grid 1-6 at the Bloomfield Ranch site, just north of the "grassy knoll". Two other, less well-defined and more problematic, features are located in the depression north of the Miller house and to the east in the agricultural field.

We suggest that subsurface testing is warranted at least for the Miller Cemetery Grid 1-4 anomaly and the Bloomfield Ranch Grid 1-6 anomaly to determine if they are associated with historic structures. Lower priority targets for testing are the Bloomfield Ranch Grid 1-5 and Grid 1-2. The overlay of modern objects and features at the Bloomfield Ranch house made a significant contribution to the geophysical anomalies at this site and may have obscured signatures from the older Mariano Castro adobe. On the other hand, the Miller Cemetery site is relatively less disturbed and yielded both geophysical anomalies and surface potter that is consistent with a Spanish period occupation.

References

Anonymous
1999 Surfer. Version 7.0. Golden Software, Inc. Golden, CO.

Conyers, Lawrence B., and Dean Goodman
1997 Ground-penetrating Radar: An Introduction for Archaeologists. Walnut Creek, CA: Altamira Press.

Conyers, Lawrence B. and Jeffrey E. Lucius
1996 Velocity Analysis in Archaeological Ground-penetrating Radar Studies. Archaeological Prospection. 3: 25-38.

Costello, Julia
2002 Extended Phase I Research: Field Preparation for the Geophysical Survey of Selected Portions of the Miller Cemetery (P-43-000315; CA-SCl-308/H) and Bloomfield Farm (P-43-111077, CA-SCl-697H) Sites. Report on file Caltrans District 05, San Luis Obispo, CA.

Reynolds, J.M.
1997 An Introduction to Applied and Environmental Geophysics. Chichester: John Wiley and Sons.

Wee, Stephen R.
2002 Historic Background Report: Castro Adobe Site. Davis, CA: JRP Historical Consulting Services.

Appendix I – Selected GPR Vertical Profiles

The first profile (File 1) from each grid was collected beginning at the grid origin (illustrated in report Figures 1 and 2). Subsequent profiles (File 5, etc.) were selected at 2m line spacing and referenced to the same grid origin.

Las Animas GPR Grid #1-1

07_10_02: File 1

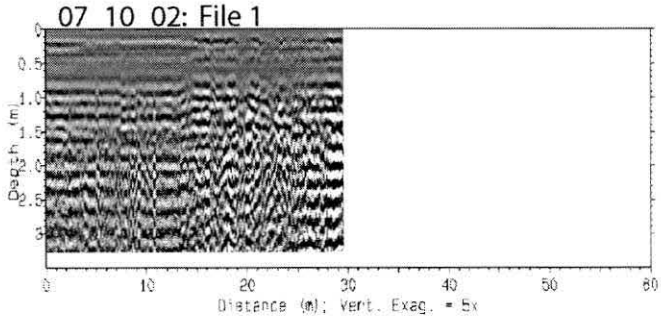

07_10_02: File 21

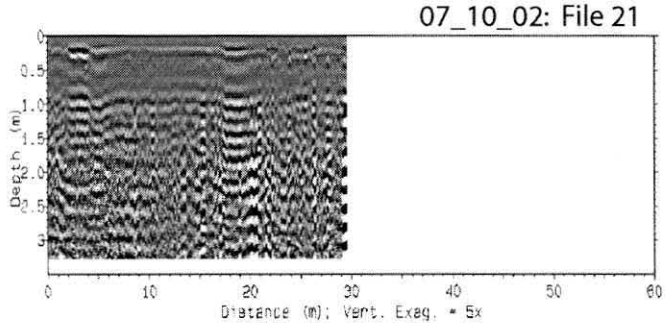

07_10_02: File 5

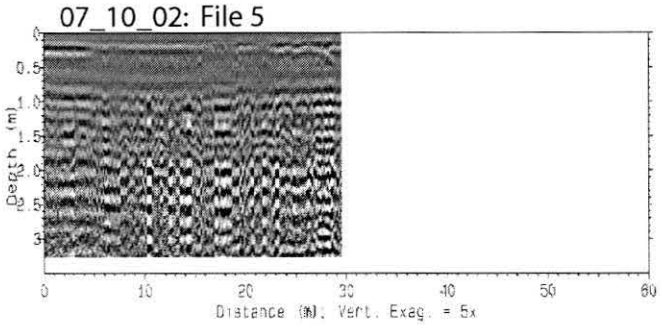

07_10_02: File 25

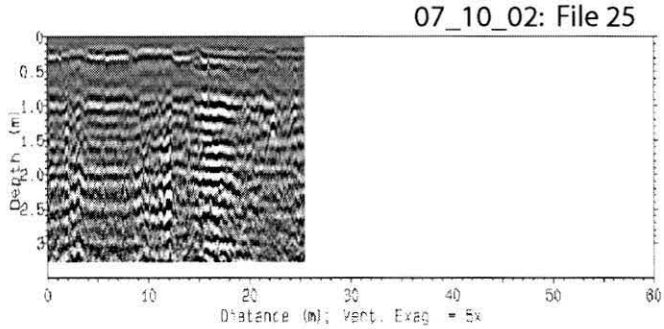

07_10_02: File 9

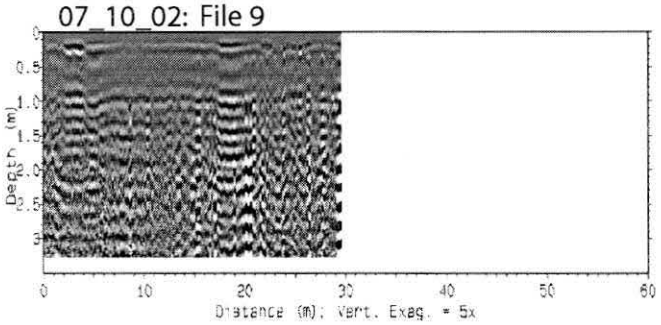

07_10_02: File 29

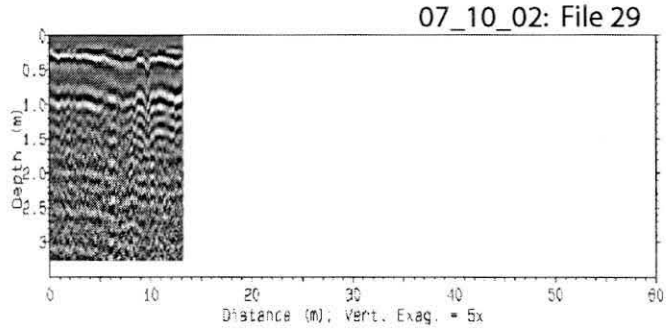

07_10_02: File 13

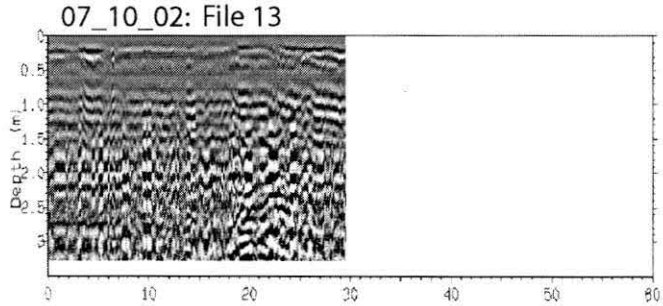

07_10_02: File 33

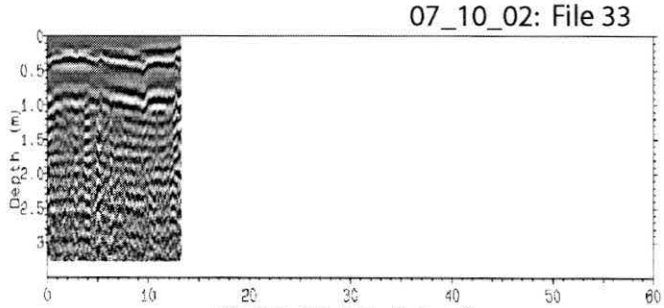

07_10_02: File 17

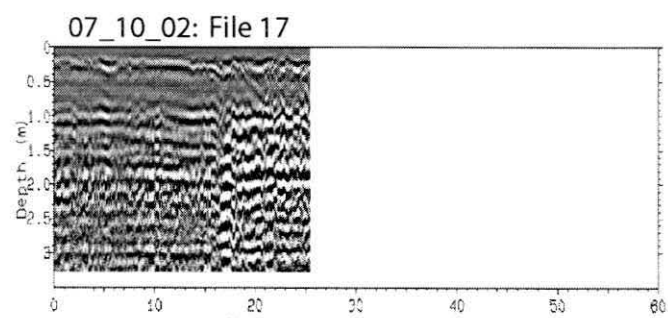

07_10_02: File 49

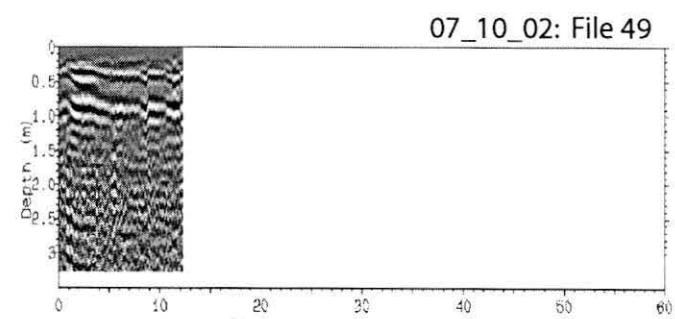

Las Animas GPR Grid #1-1

07_10_02: File 37

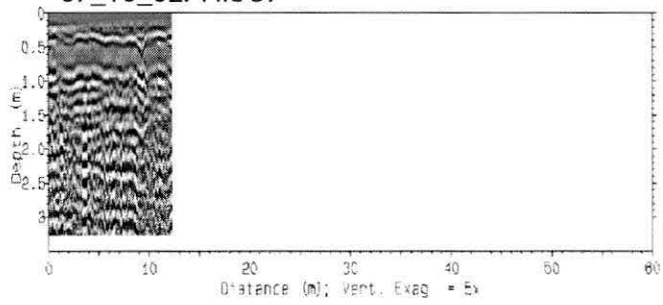

07_10_02: File 61

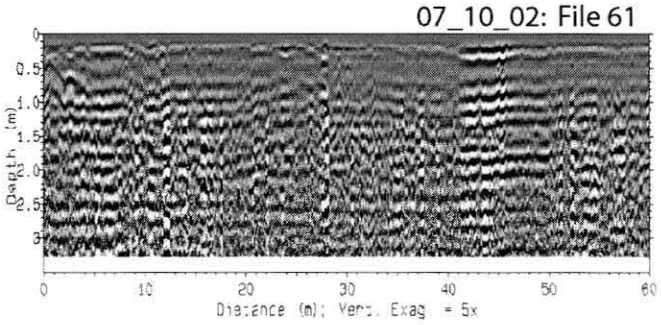

07_10_02: File 41

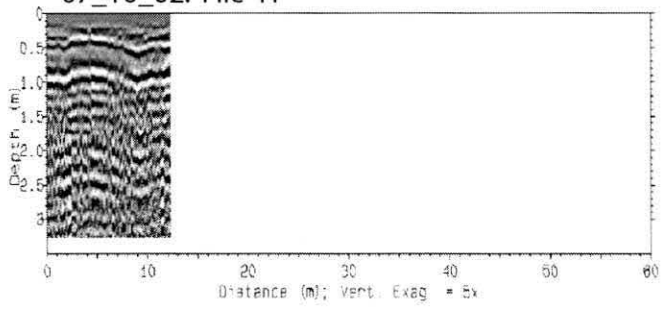

07_10_02: File 65

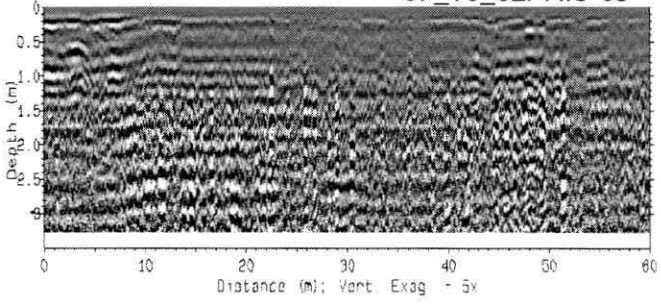

07_10_02: File 45

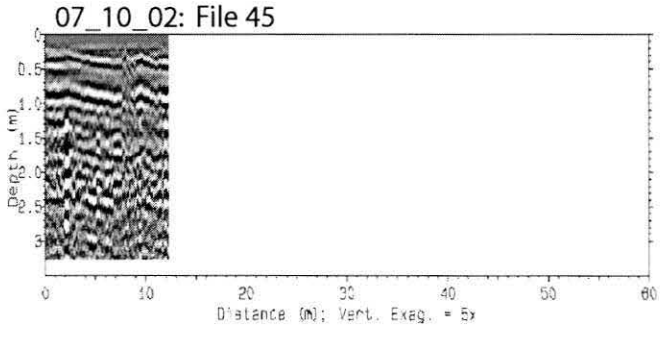

07_10_02: File 69

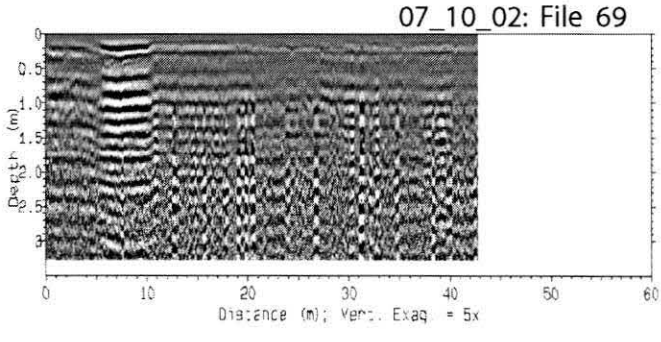

07_10_02: File 53

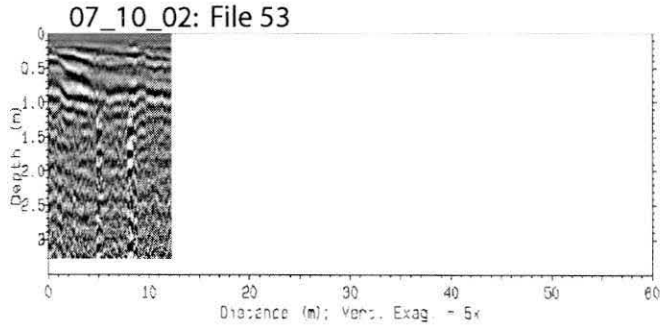

07_10_02: File 73

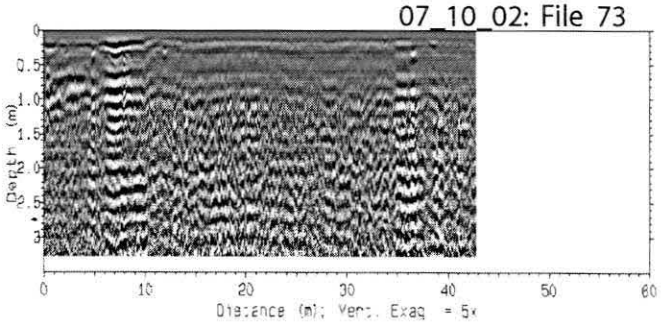

07_10_02: File 58

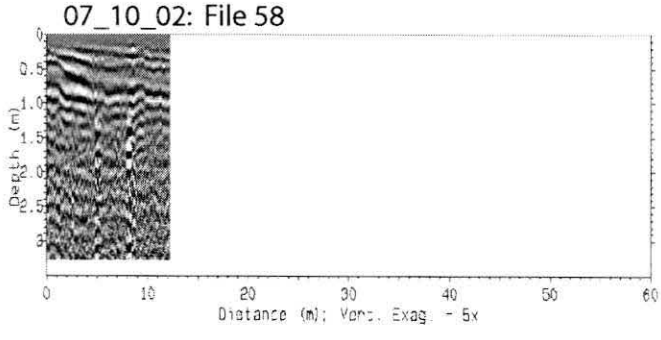

Las Animas GPR Grid #1-2

07_10_02.001: File 1

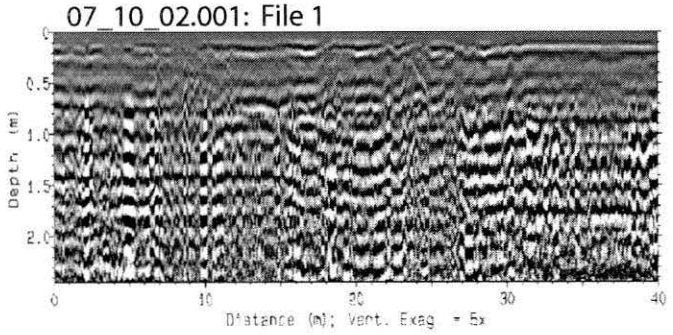

07_10_02.001: File 5

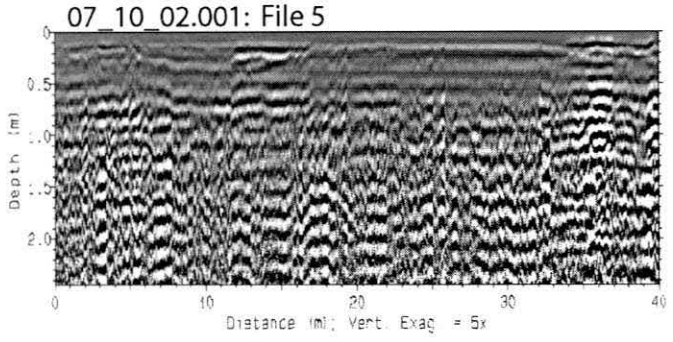

07_10_02.001: File 9

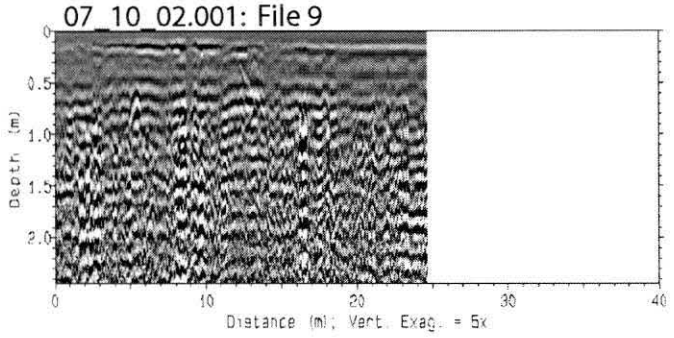

07_10_02.001: File 13

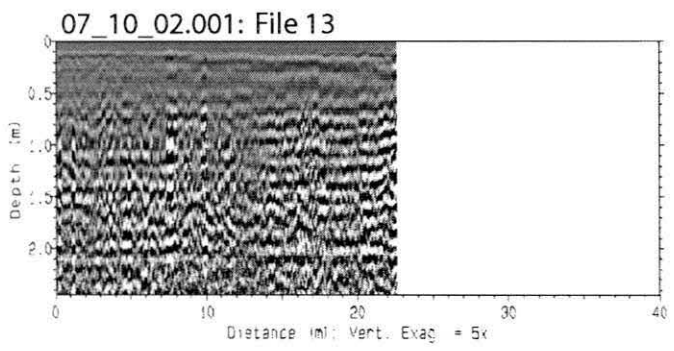

07_10_02.001: File 17

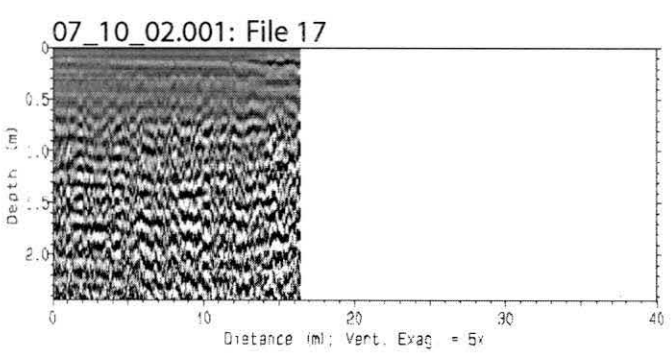

Las Animas GPR Grid #1-3

07_11_02: File 1

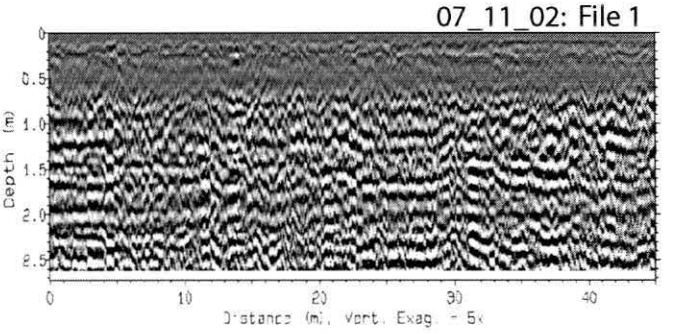

07_11_02: File 5

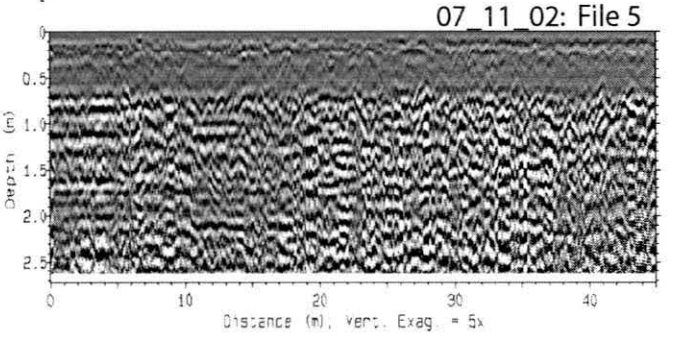

07_11_02: File 9

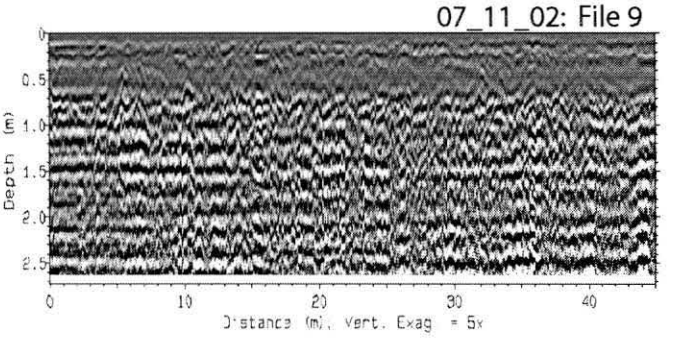

07_11_02: File 13

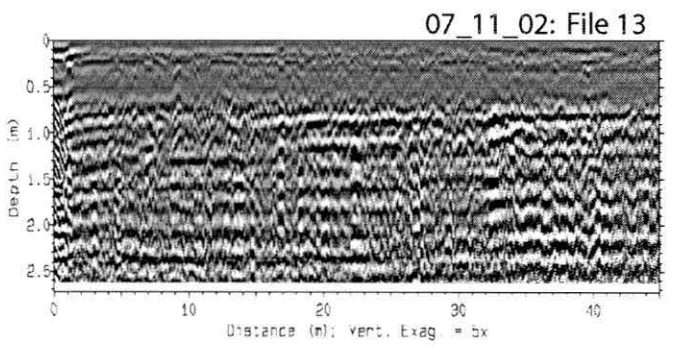

07_11_02: File 17

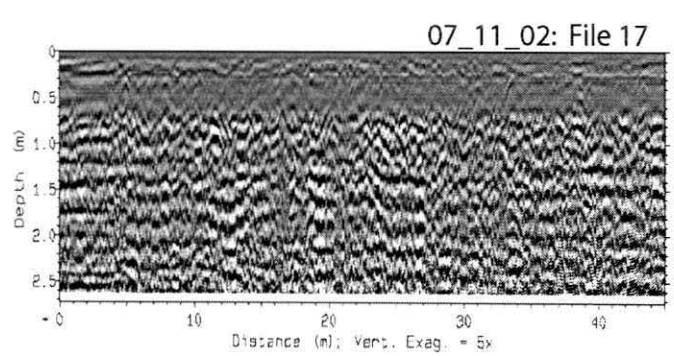

Las Animas GPR Grid #1-3

07_11_02: File 21

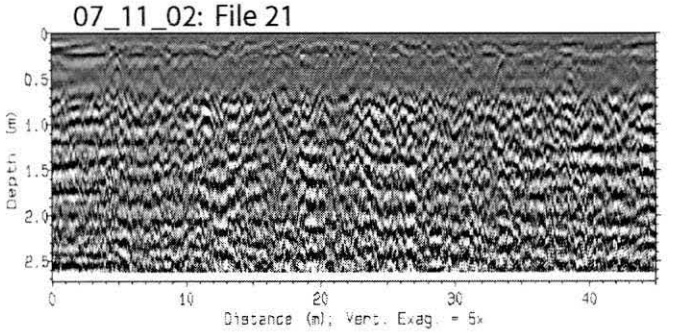

07_11_02: File 41

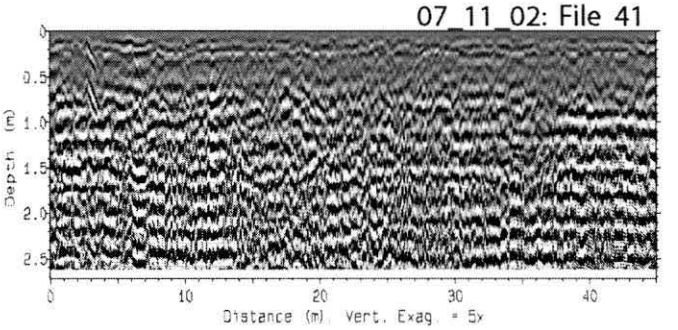

07_11_02: File 25

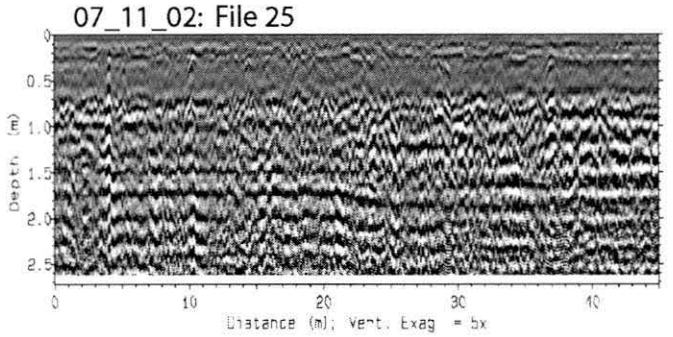

07_11_02: File 45

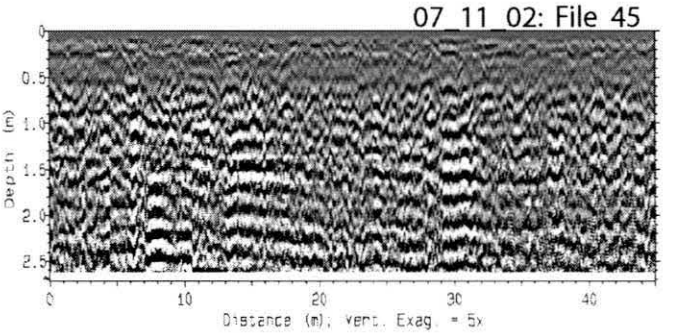

07_11_02: File 29

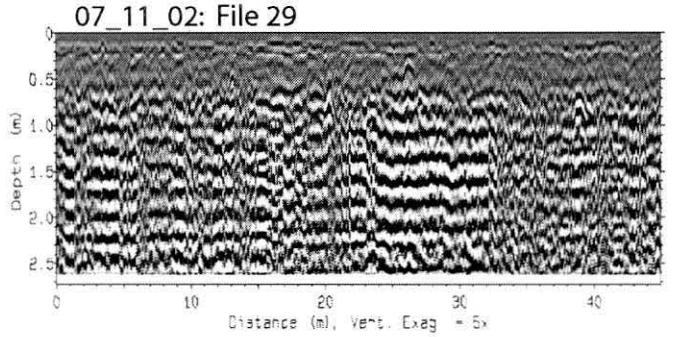

07_11_02: File 49

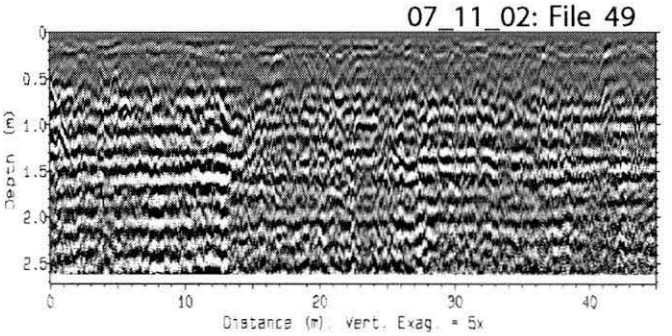

07_11_02: File 33

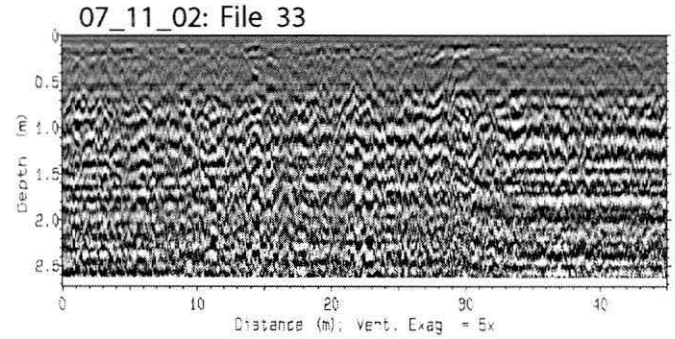

07_11_02: File 37

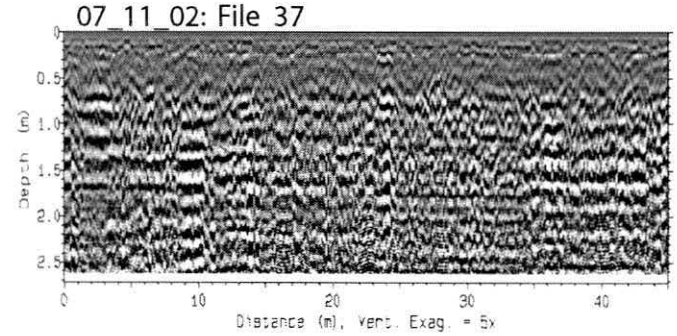

Las Animas GPR Grid #1-4

07_11_02.001: File 1

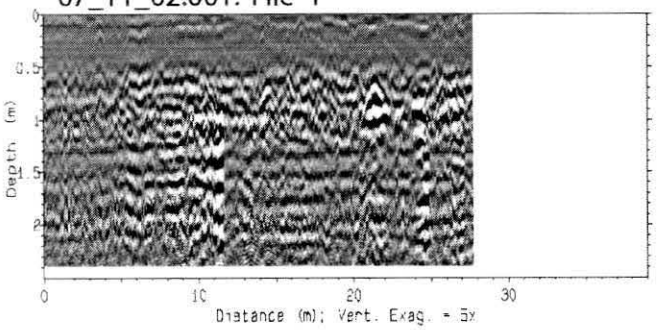

07_11_02.001: File 21

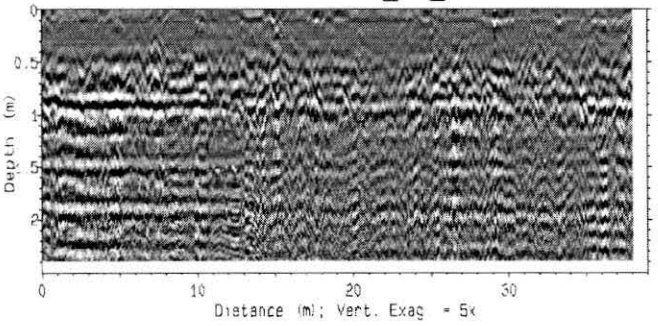

07_11_02.001: File 5

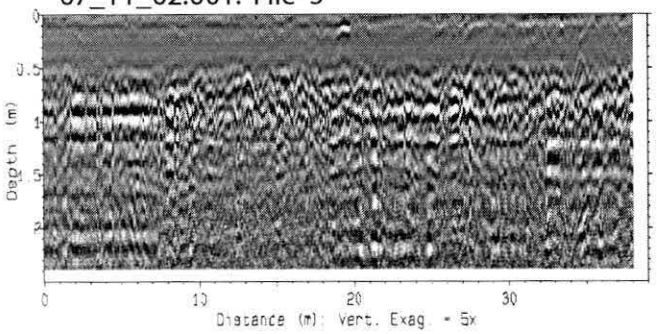

07_11_02.001: File 25

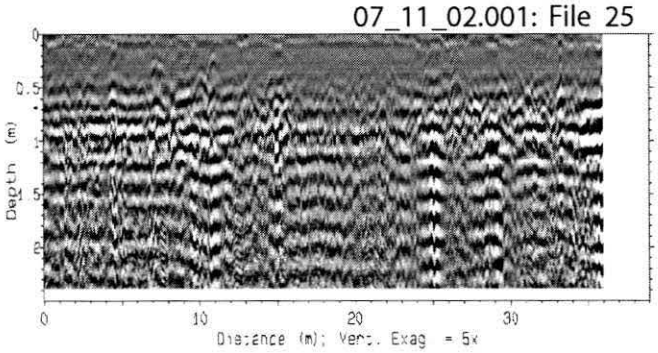

07_11_02.001: File 9

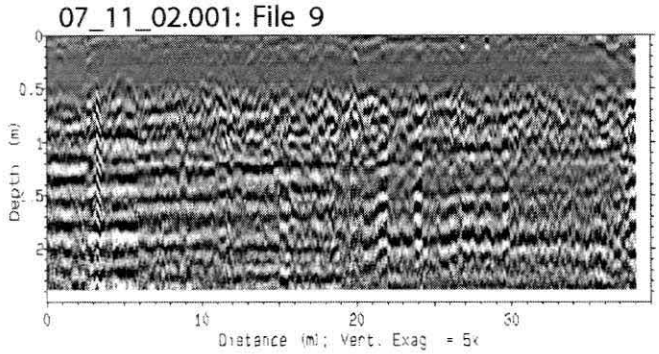

07_11_02.001: File 29

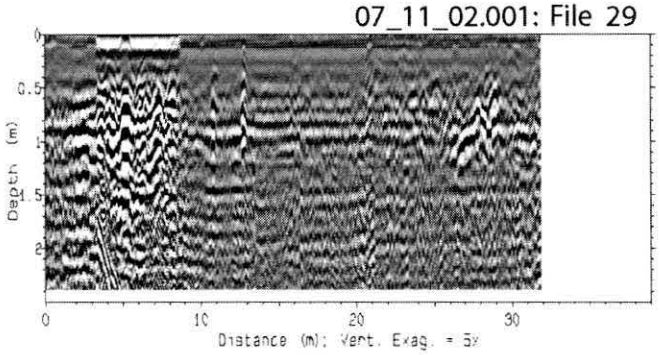

07_11_02.001: File 13

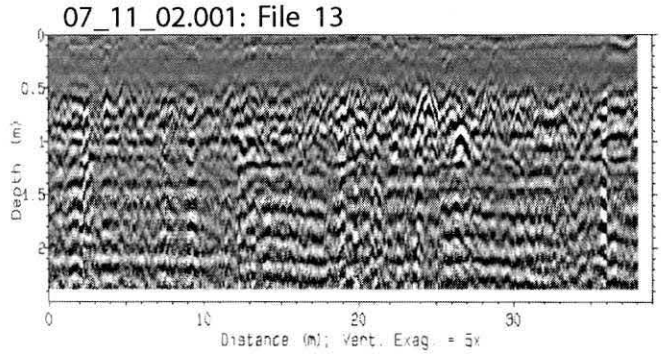

07_11_02.001: File 33

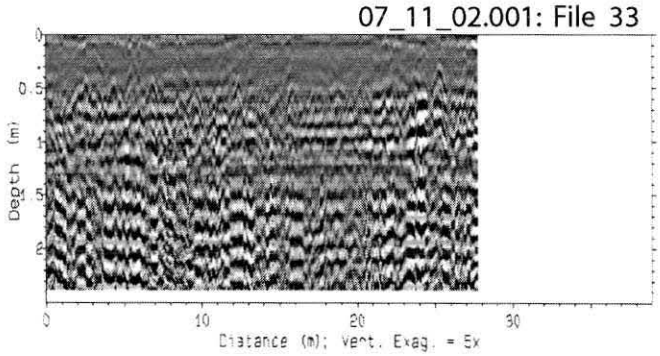

07_11_02.001: File 17

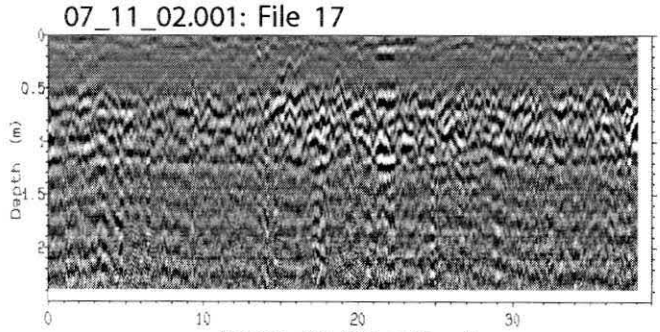

07_11_02.001: File 37

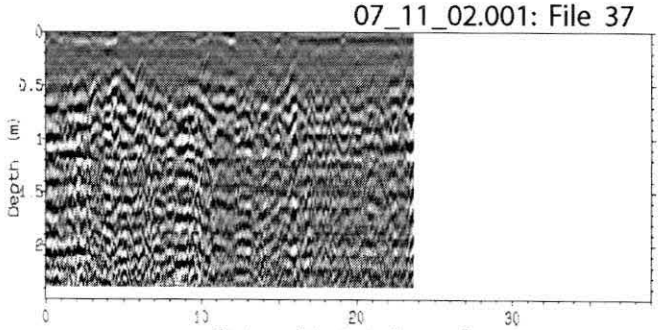

Las Animas GPR Grid #1-5

07_12_02: File 1

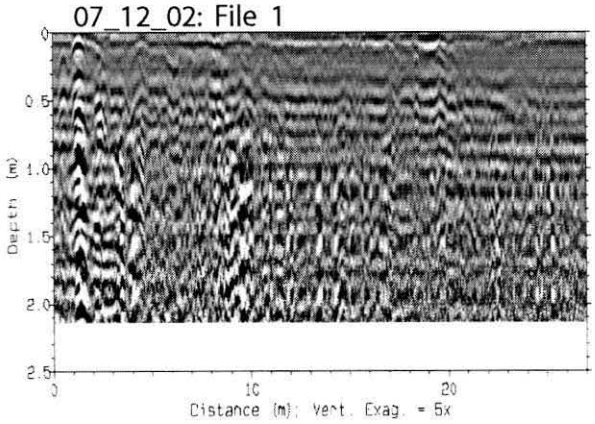

07_12_02: File 17

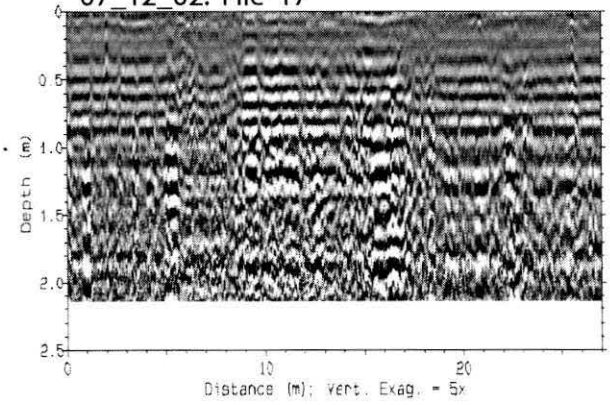

07_12_02: File 5

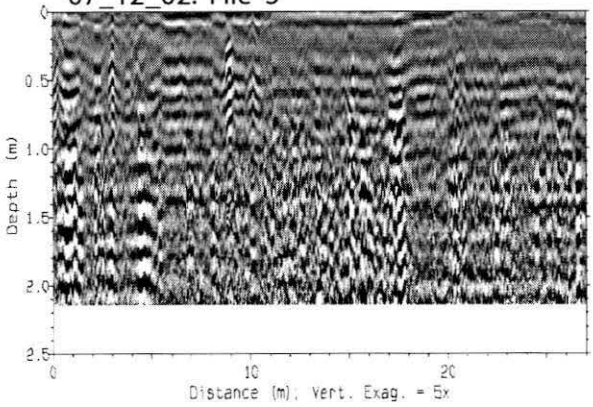

07_12_02: File 21

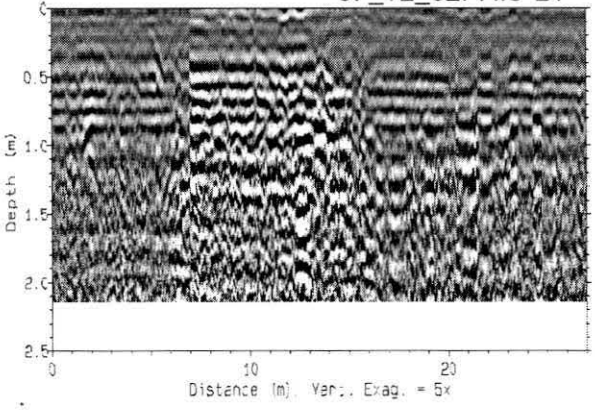

07_12_02: File 9

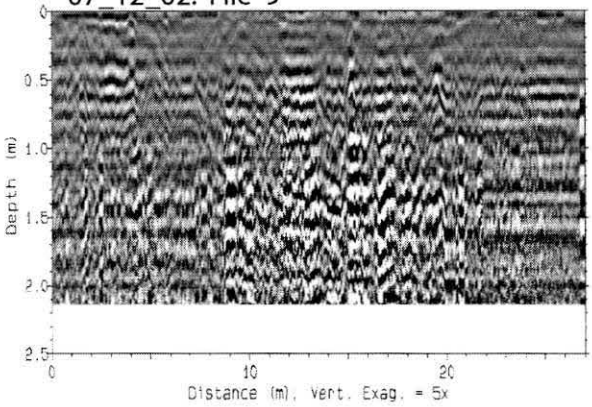

07_12_02: File 25

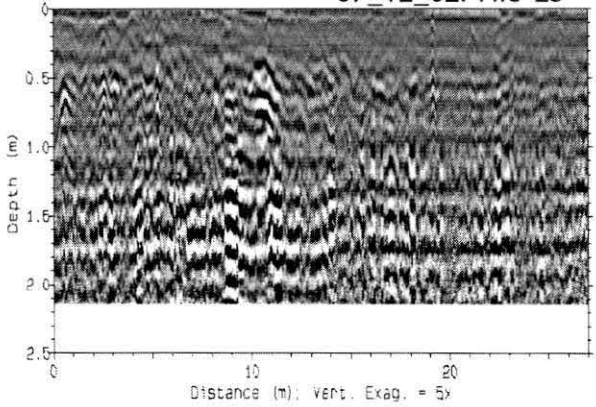

07_12_02: File 13

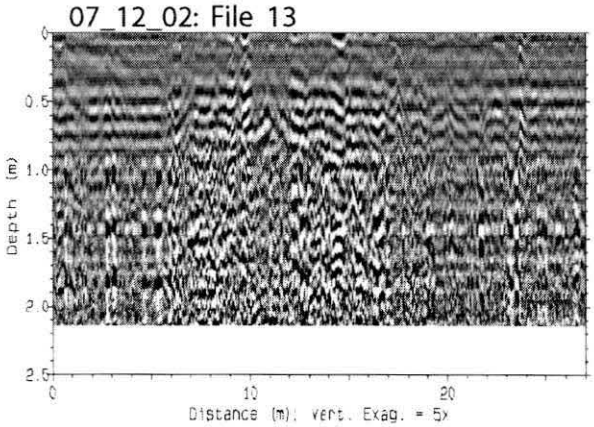

07_12_02: File 29

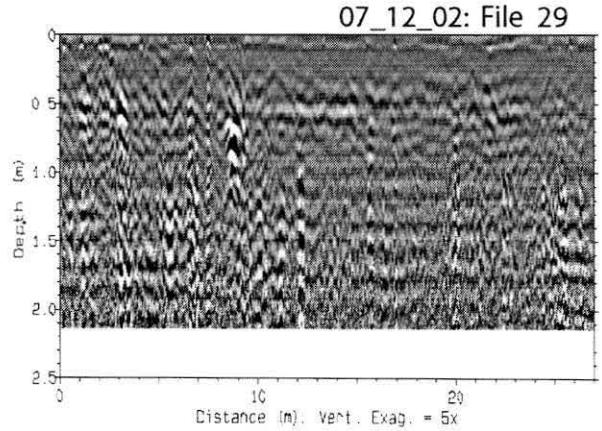

Las Animas GPR Grid #1-6

07_12_02.001: File 41

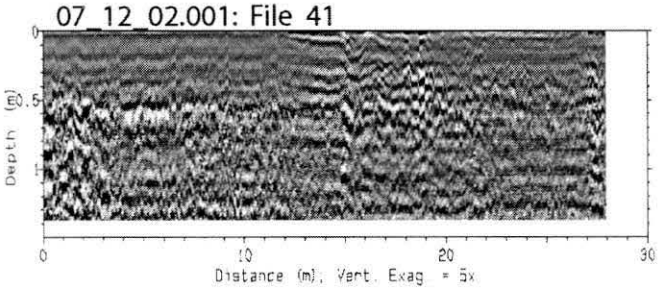

07_12_02.001: File 65

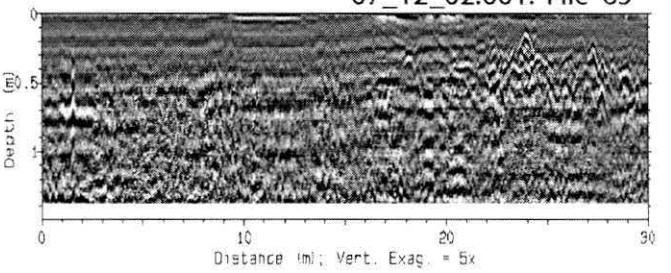

07_12_02.001: File 45

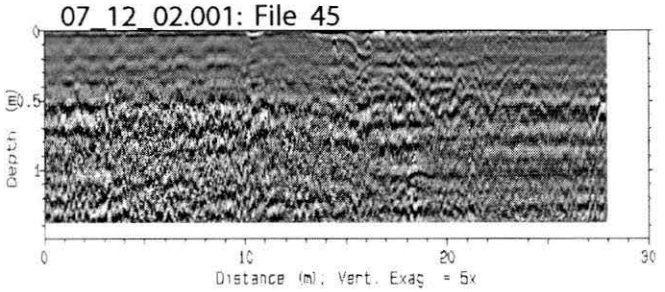

07_12_02.001: File 69

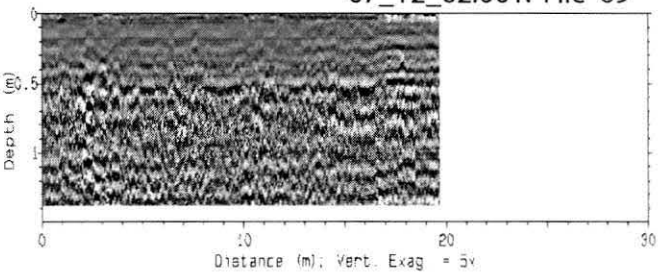

07_12_02.001: File 49

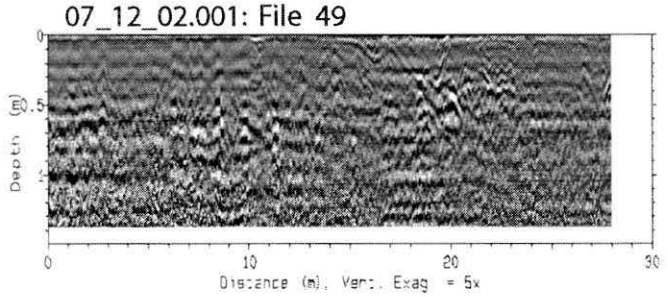

07_12_02.001: File 73

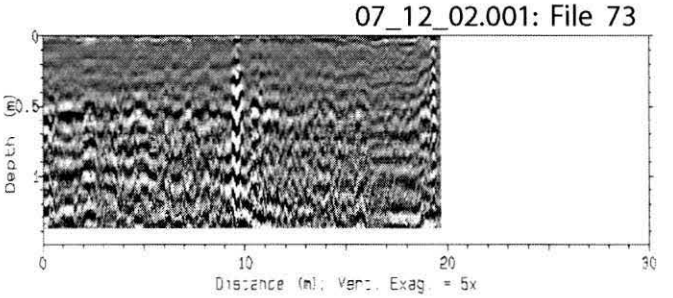

07_12_02.001: File 53

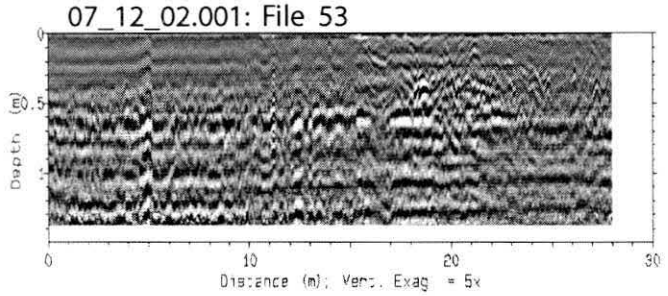

07_12_02.001: File 77

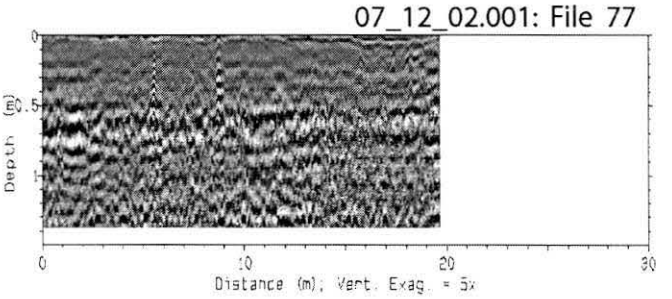

07_12_02.001: File 57

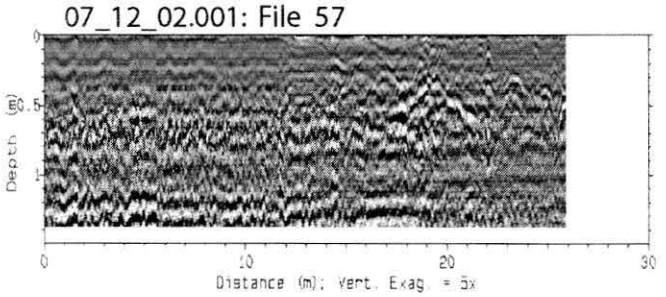

07_12_02.001: File 81

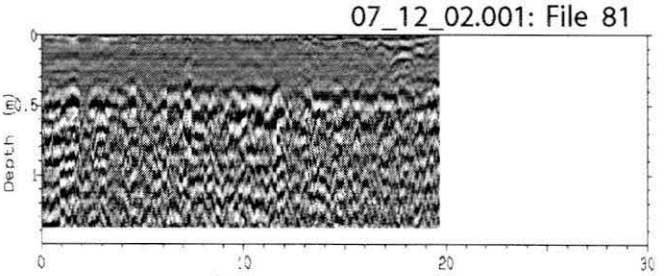

07_12_02.001: File 61

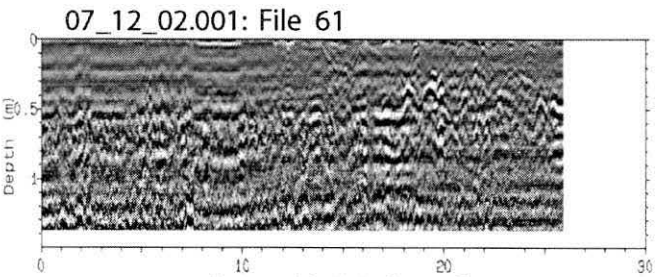

Las Animas Grid #1-6

07_12_02.001: File 2

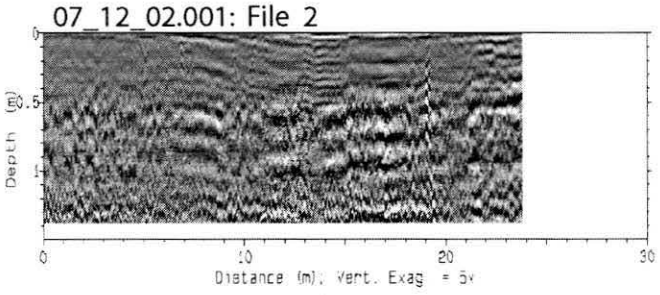

07_12_02.001: File 21

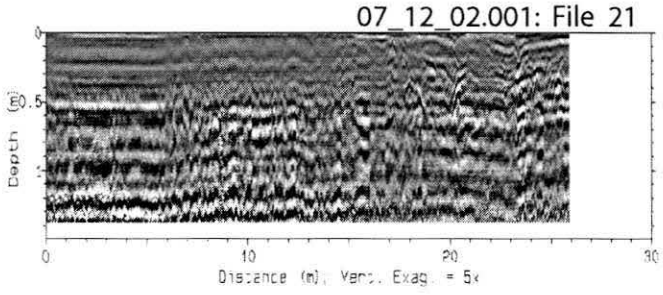

07_12_02.001: File 5

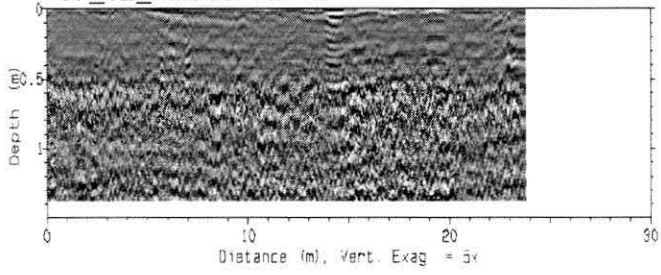

07_12_02.001: File 25

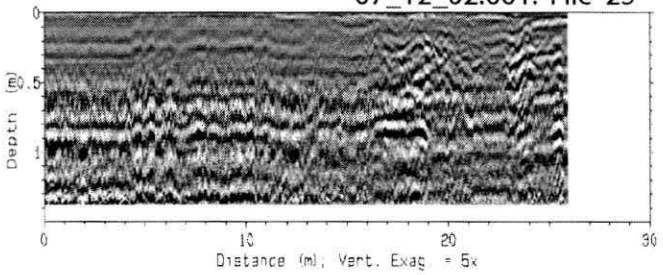

07_12_02.001: File 10

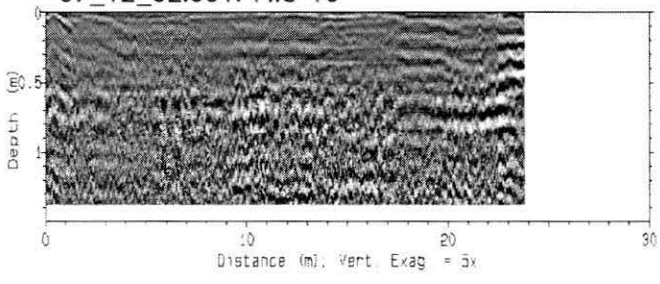

07_12_02.001: File 29

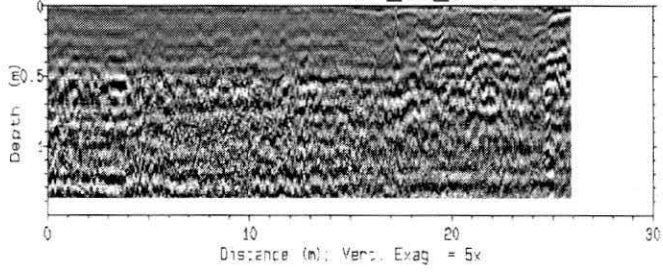

07_12_02.001: File 13

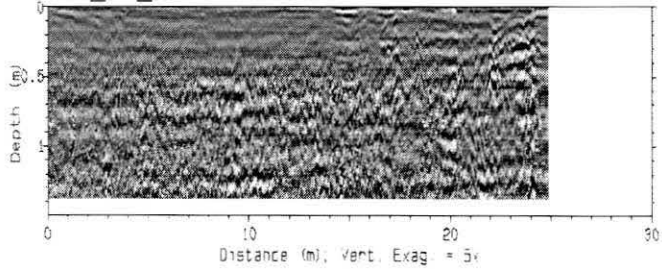

07_12_02.001: File 33

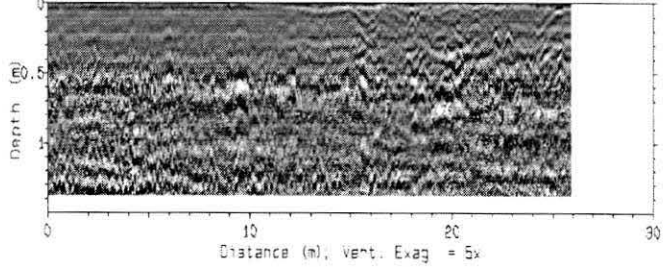

07_12_02.001: File 17

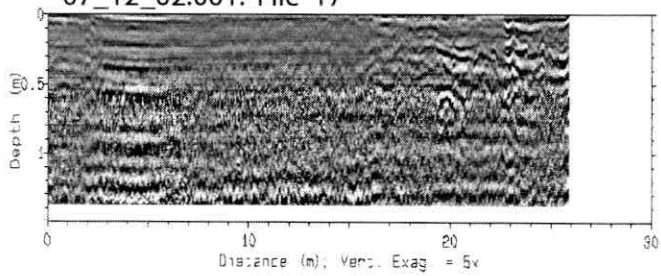

07_12_02.001: File 37

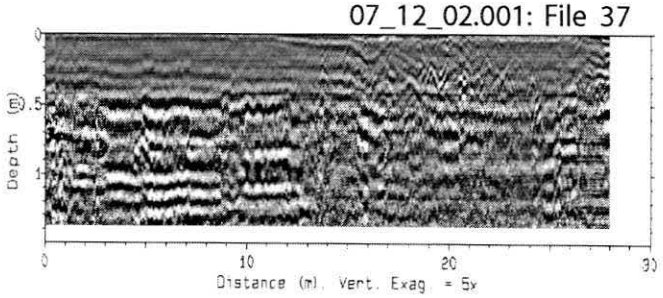

Las Animas GPR Grid #1-7

07_13_02: File 1

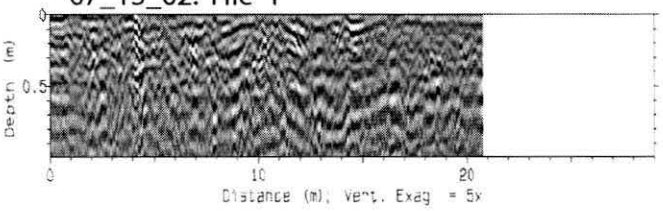

07_13_02: File 29

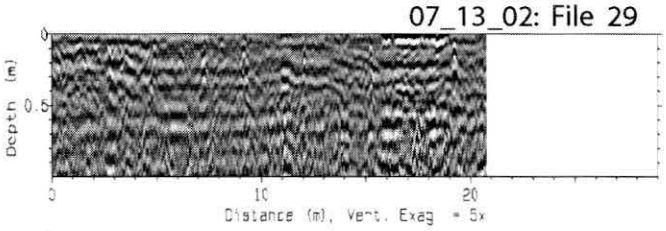

07_13_02: File 5

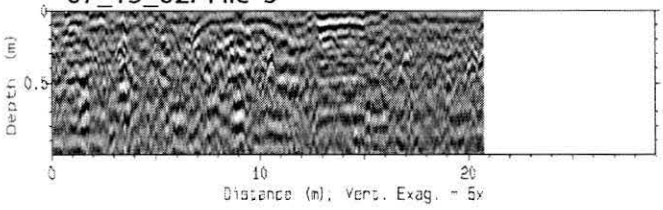

07_13_02: File 33

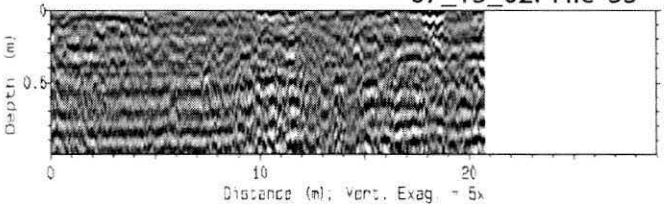

07_13_02: File 9

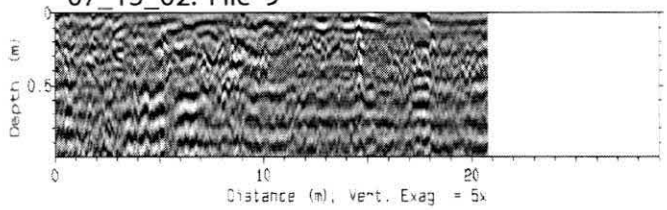

07_13_02: File 38

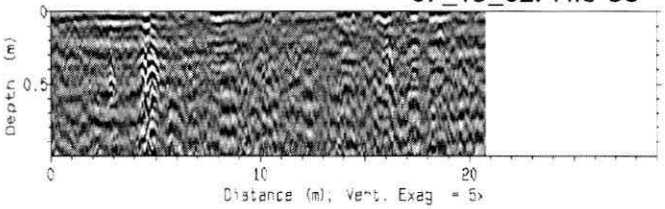

07_13_02: File 13

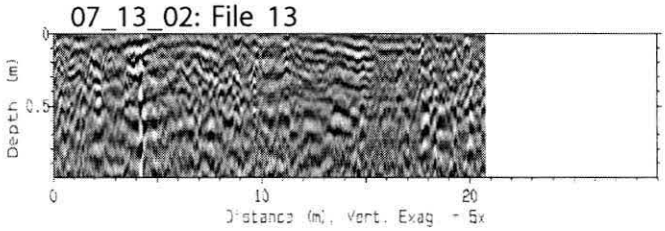

07_13_02: File 41

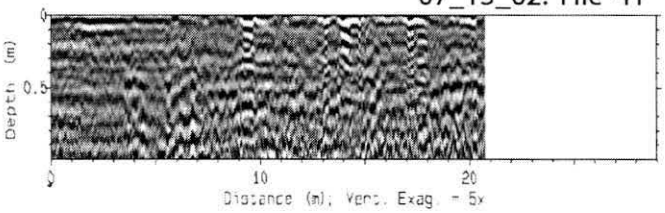

07_13_02: File 17

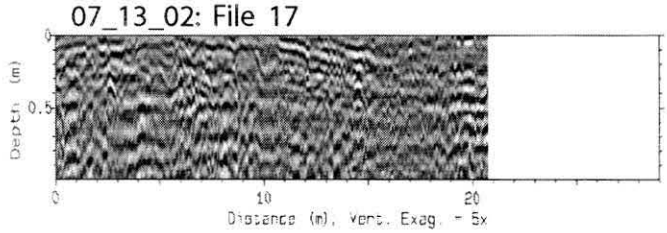

07_13_02: File 45

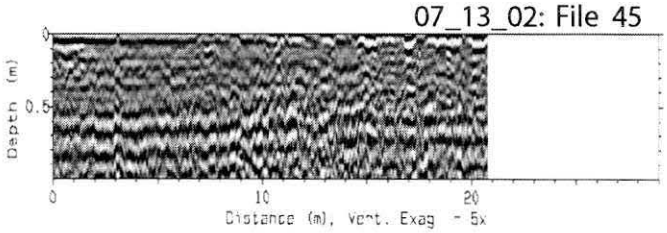

07_13_02: File 21

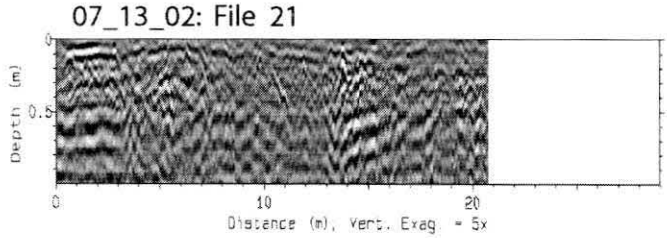

07_13_02: File 49

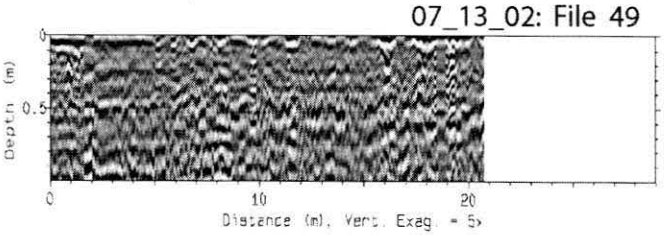

07_13_02: File 25

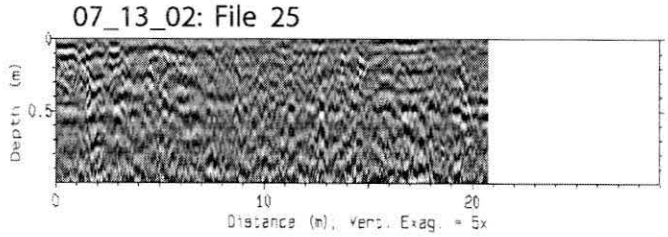

07_13_02: File 53

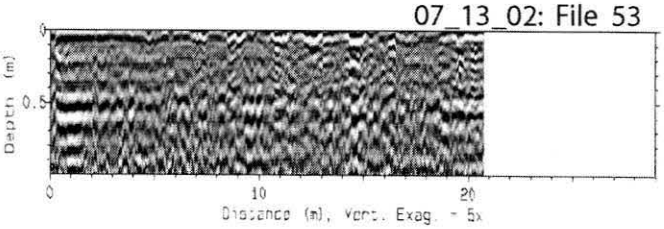

Las Animas GPR Grid #1-7

07_13_02: File 57

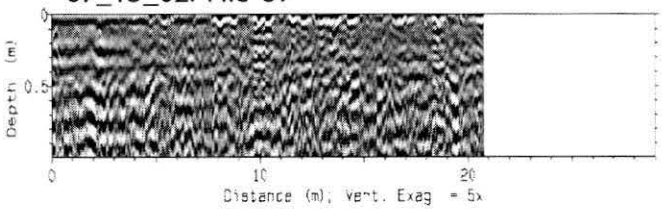

07_13_02: File 61

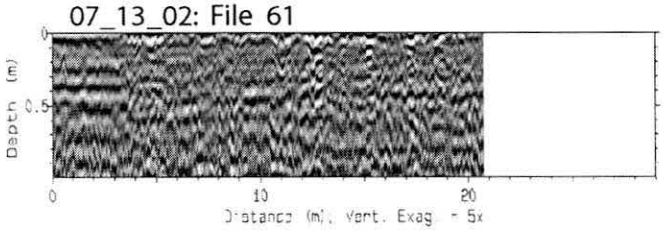

07_13_02: File 65

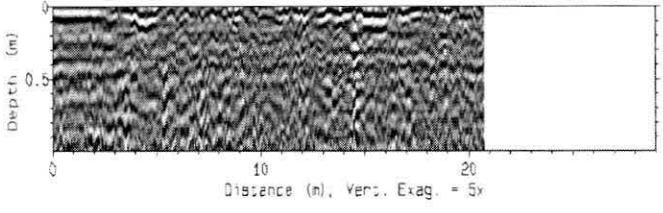

07_13_02: File 69

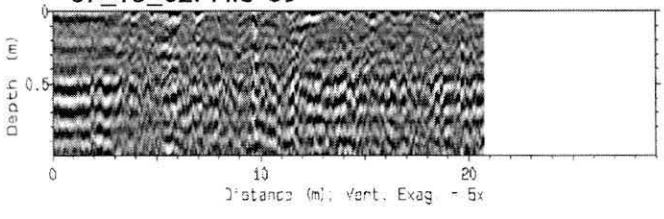

07_13_02: File 73

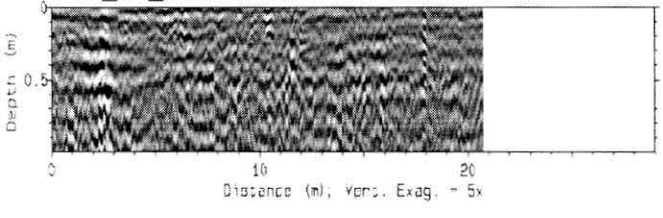

07_13_02: File 77

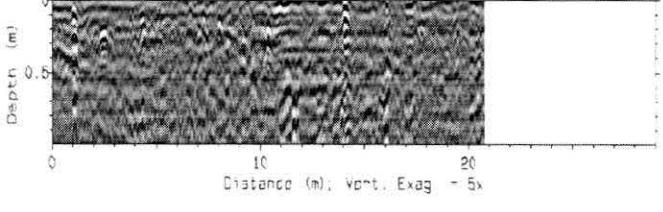

07_13_02: File 81

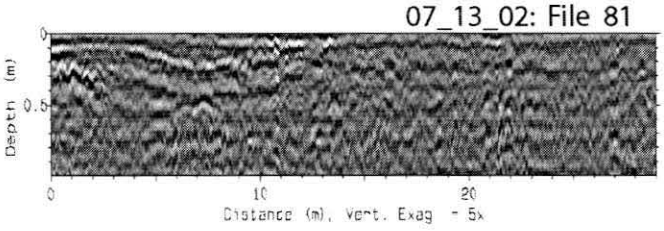

07_13_02: File 85

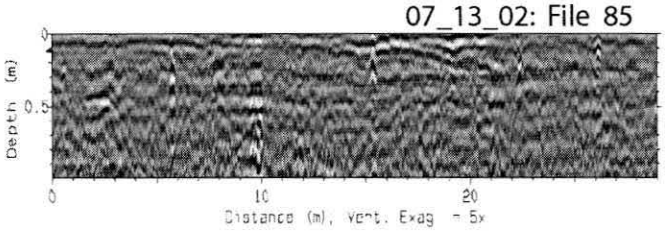

07_13_02: File 89

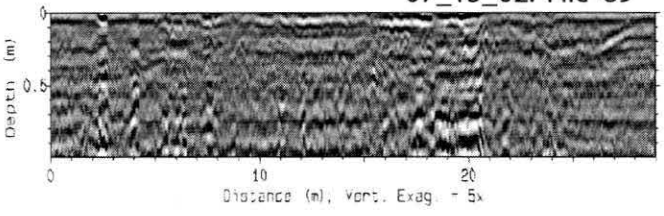

07_13_02: File 93

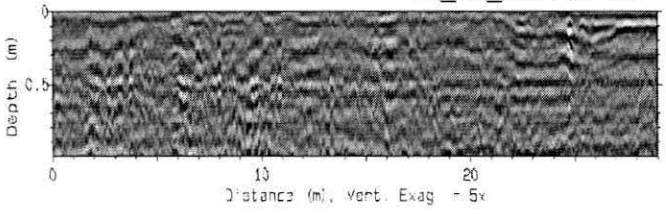

07_13_02: File 97

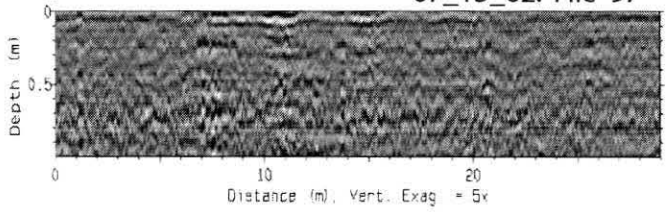

07_13_02: File 101

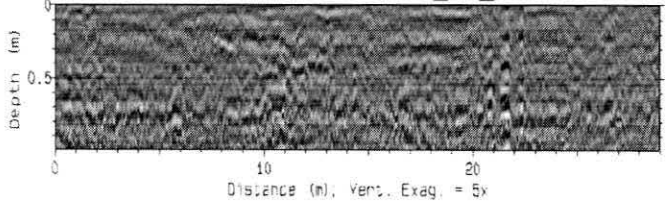

07_13_02: File 105

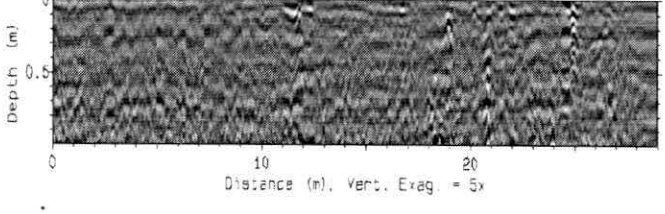

Las Animas GPR Grid #2-1

10_18_02: File 1

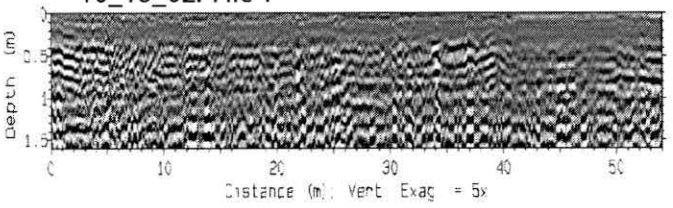

10_18_02: File 17

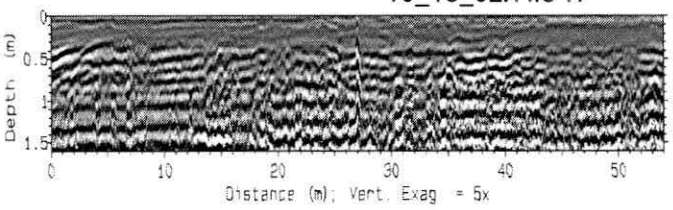

10_18_02: File 5

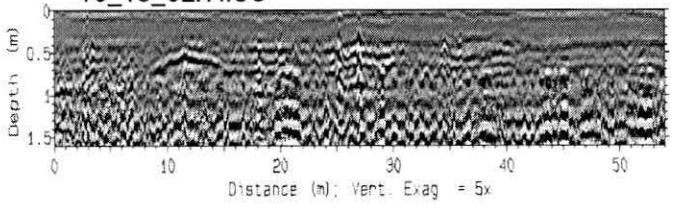

10_18_02: File 21

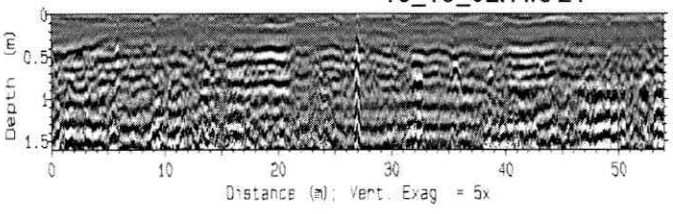

10_18_02: File 9

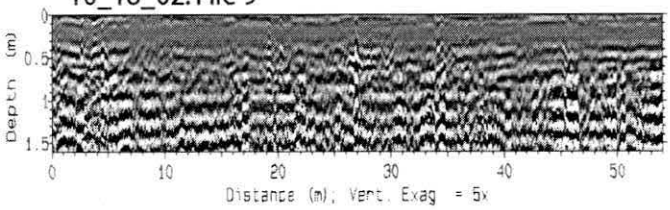

10_18_02: File 25

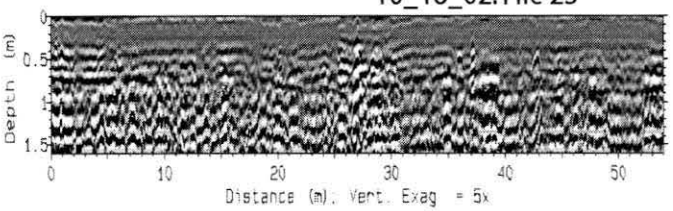

10_18_02: File 13

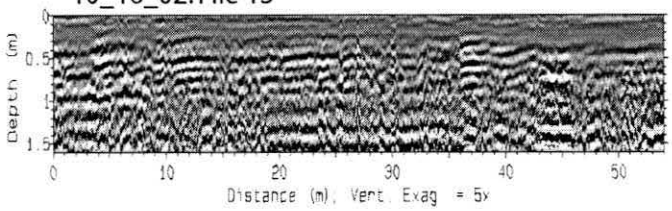

10_18_02: File 29

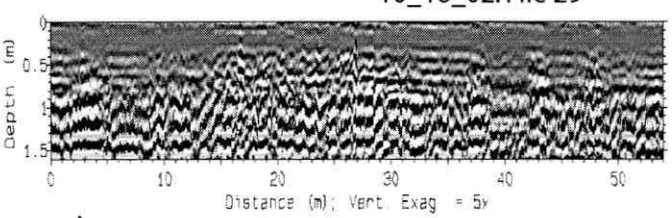

Las Animas GPR Grid #2-2

10_18_02.001: File 1

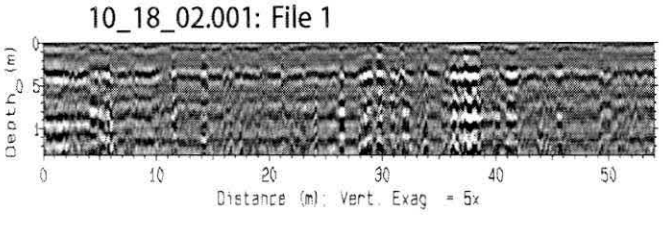

10_18_02.001: File 13

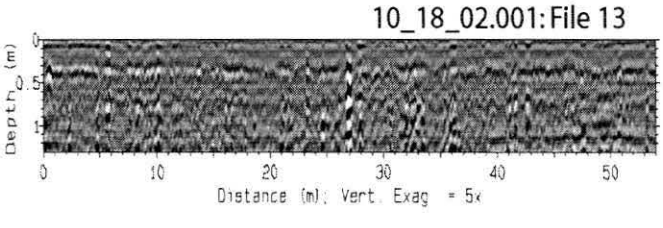

10_18_02.001: File 5

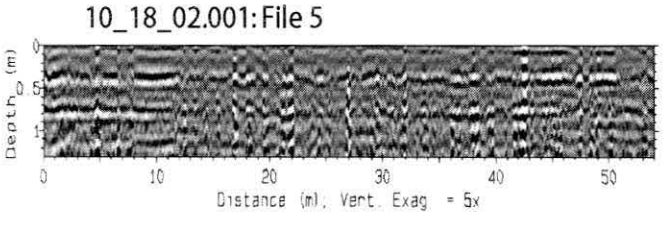

10_18_02.001: File 17

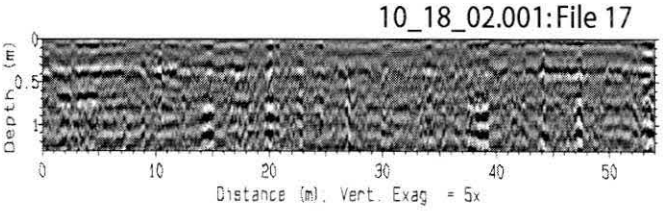

10_18_02.001: File 9

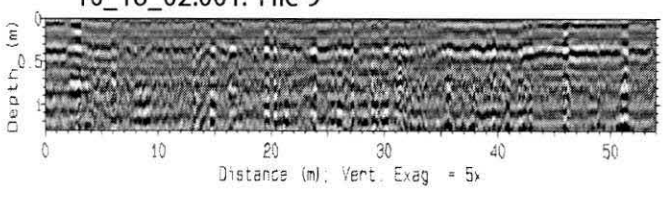

10_18_02.001: File 21

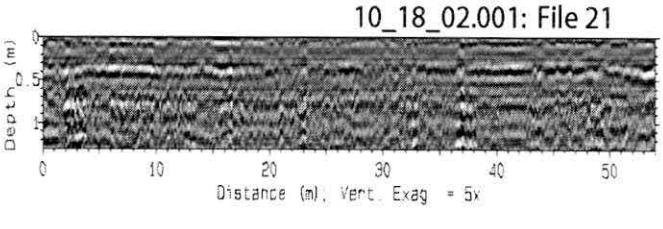

10_18_02.001: File 25

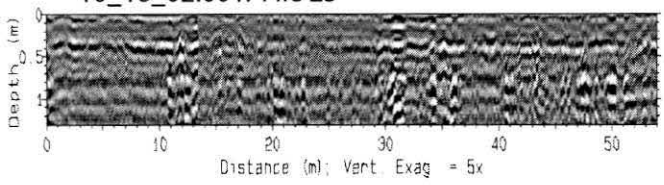

Las Animas GPR Grid #2-3

10_19_02: File 1

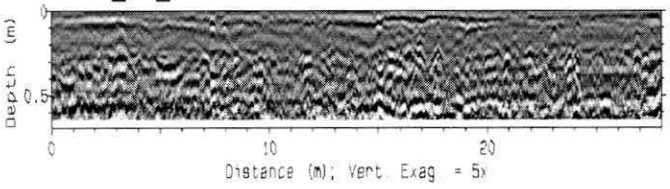

10_19_02:File 13

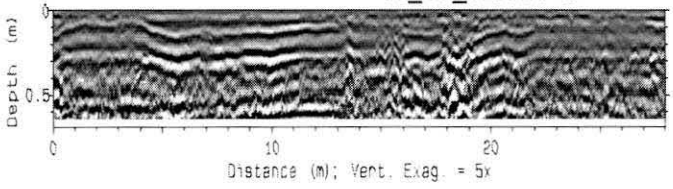

10_19_02:File 5

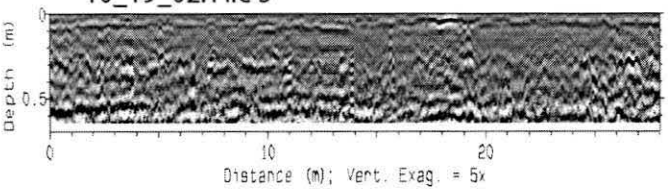

10_19_02:File 17

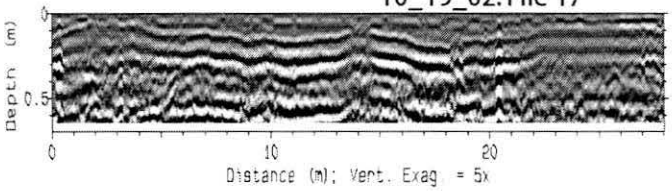

10_19_02:File 9

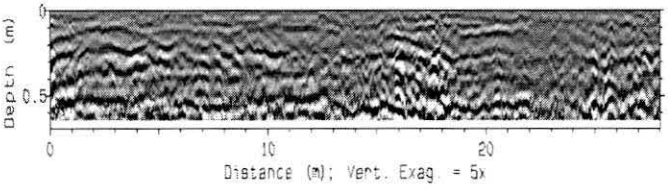

10_19_02:File 21

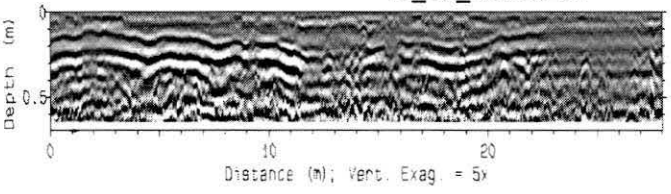

Las Animas GPR Grid #2-4

10_19_02.001: File 1

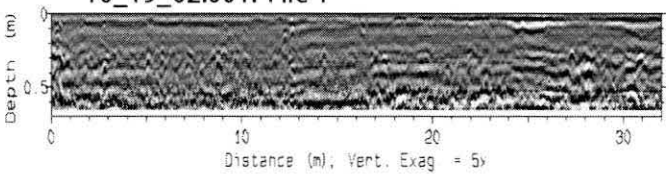

10_19_02.001: File 14

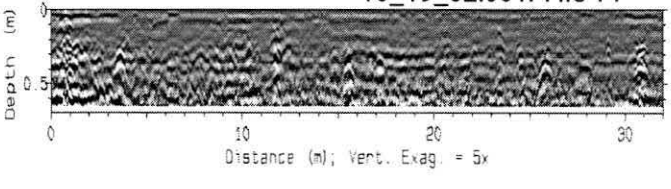

10_19_02.001:File 5

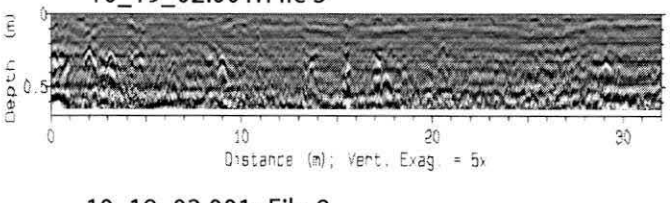

10_19_02.001:File 17

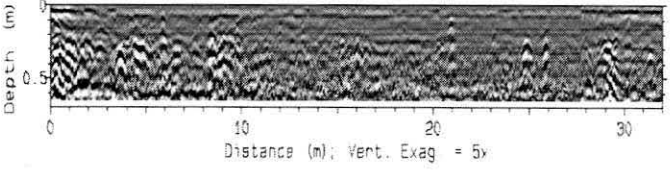

10_19_02.001: File 9

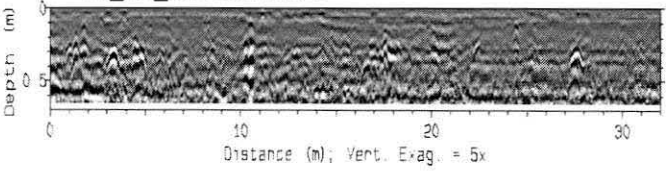

10_19_02.001:File 21

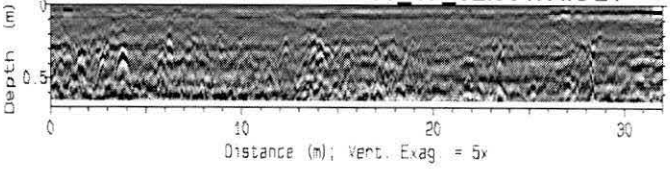

Las Animas GPR Grid #2-5

10_19_02.002: File 1

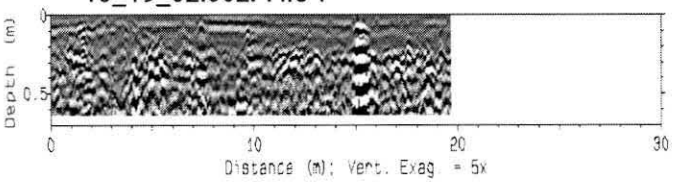

10_19_02.002: File 17

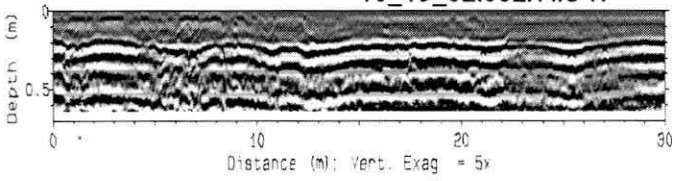

10_19_02.002: File 5

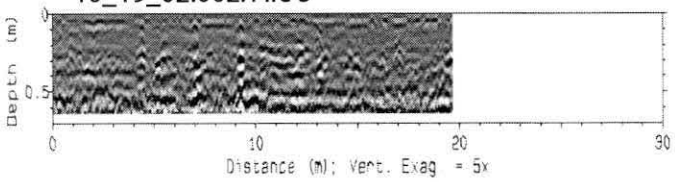

10_19_02.002: File 21

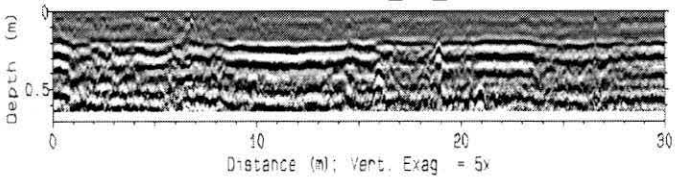

10_19_02.002: File 9

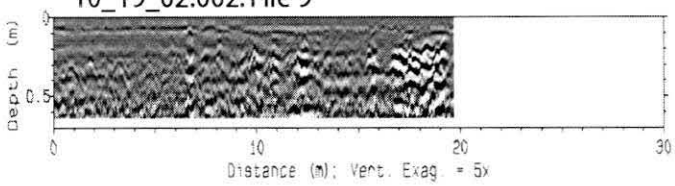

10_19_02.002: File 25

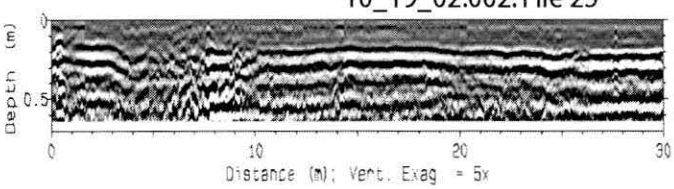

10_19_02.002: File 13

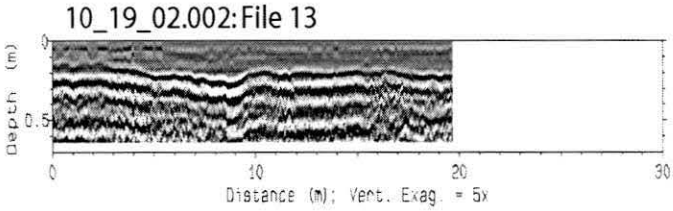

Las Animas GPR Grid #2-6

10_19_02.003: File 1

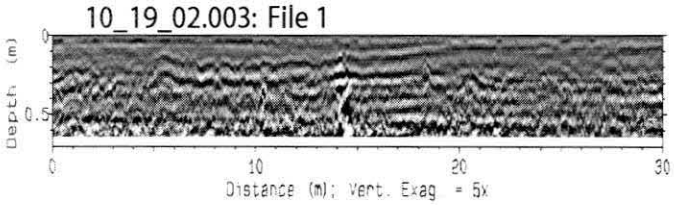

10_19_02.003: File 13

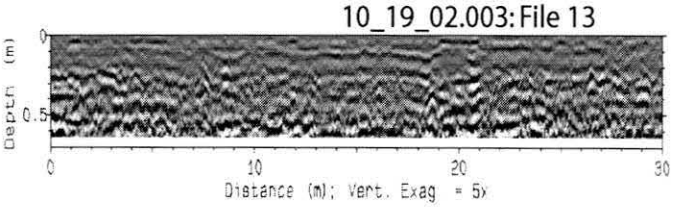

10_19_02.003: File 5

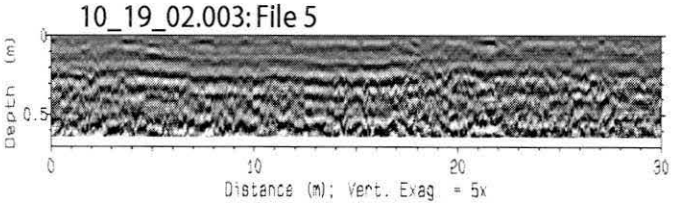

10_19_02.003: File 17

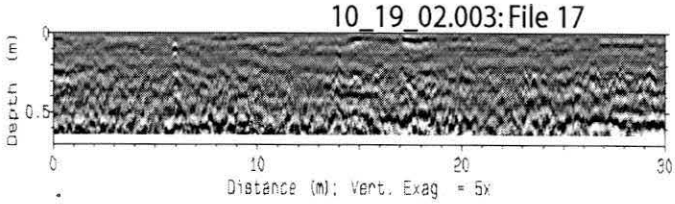

10_19_02.003: File 9

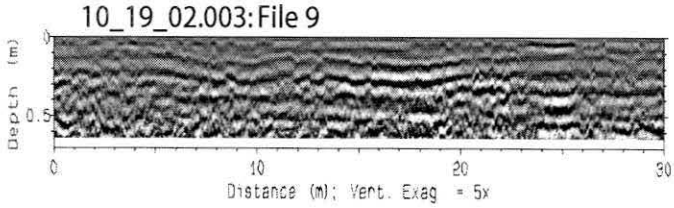

10_19_02.003: File 21